



MIMO and Smart Antennas for Mobile Broadband Systems

June 2013

CONTENTS

Introduction.....	3
1. Antenna Fundamentals	4
2. MIMO with LTE.....	7
2.1 LTE Downlink MIMO Basics.....	8
2.2 Antenna Configurations for MIMO.....	16
2.3 Performance of the various antenna configurations	22
2.4 An Analysis of Antenna Configurations for 4x2 and 4x4 MIMO.....	24
2.5 Antenna Array Calibration	27
Summary	35
Definitions and Acronyms	36
References	40
Acknowledgements	42

INTRODUCTION

Wireless traffic in the United States has nearly doubled since the last publication of this white paper in 2012 and global mobile data traffic is expected to grow 11 to 13 times over the next five years. This pressures the industry to provide increased capacity without adding the substantial costs of new base station sites. It is an immense challenge that has been addressed so far with a variety of means, not least of which has been the deployment of increasingly capable smart antenna solutions.

The LTE standard has made tremendous gains in the efficient use of Multiple-Input Multiple-Output (MIMO) and general smart antenna schemes, many of which have been increasingly applied to HSPA systems. LTE is unique in requiring as a minimum that all terminals include a second receive antenna for receive diversity and downlink MIMO support.

This white paper provides specific details of the MIMO techniques and antenna configurations that have helped meet the burgeoning growth in mobile broadband demand. It also focuses on the transmit modes (TMs) and the appropriate antenna configurations that have proven themselves in field deployments. This paper is a condensed version with some updated material from the 2012 4G Americas white paper, available for download at: www.4gamericas.org. The 2012 version provides a more expansive scope including the history, trends, and specification of antennas and ancillary equipment.

1. ANTENNA FUNDAMENTALS

Antennas are critical to all wireless communications and significant advances in their capabilities have been made in the past several decades. Figure 1 below shows the inside of a modern antenna, where we are reminded that what we refer to as an antenna consists of a number of individual antenna elements all contained within a single radome. The antenna shown below has four coaxial DIN¹ connectors serving two frequency bands each with two polarizations. The coaxial connections feed a distribution network that connects the 4 separate signals to the radiating elements. In one case, the coaxial connector feeds the +45° polarization of the 5 higher frequency band radiating elements (mounted on the circular plates) while another coaxial connection feeds the +45° polarization radiating elements in the 4 lower frequency band radiating elements. The feed network includes a variable phase shifter shown in Figure 2 that introduces a larger transmission delay to the lower elements so that the electromagnetic waves radiating from the elements will be in phase at an angle tilted down toward the ground where the mobile users are located. The tilt angle may be adjusted with a manual tilt rod or a motorized actuator controlled remotely over the AISG connection.

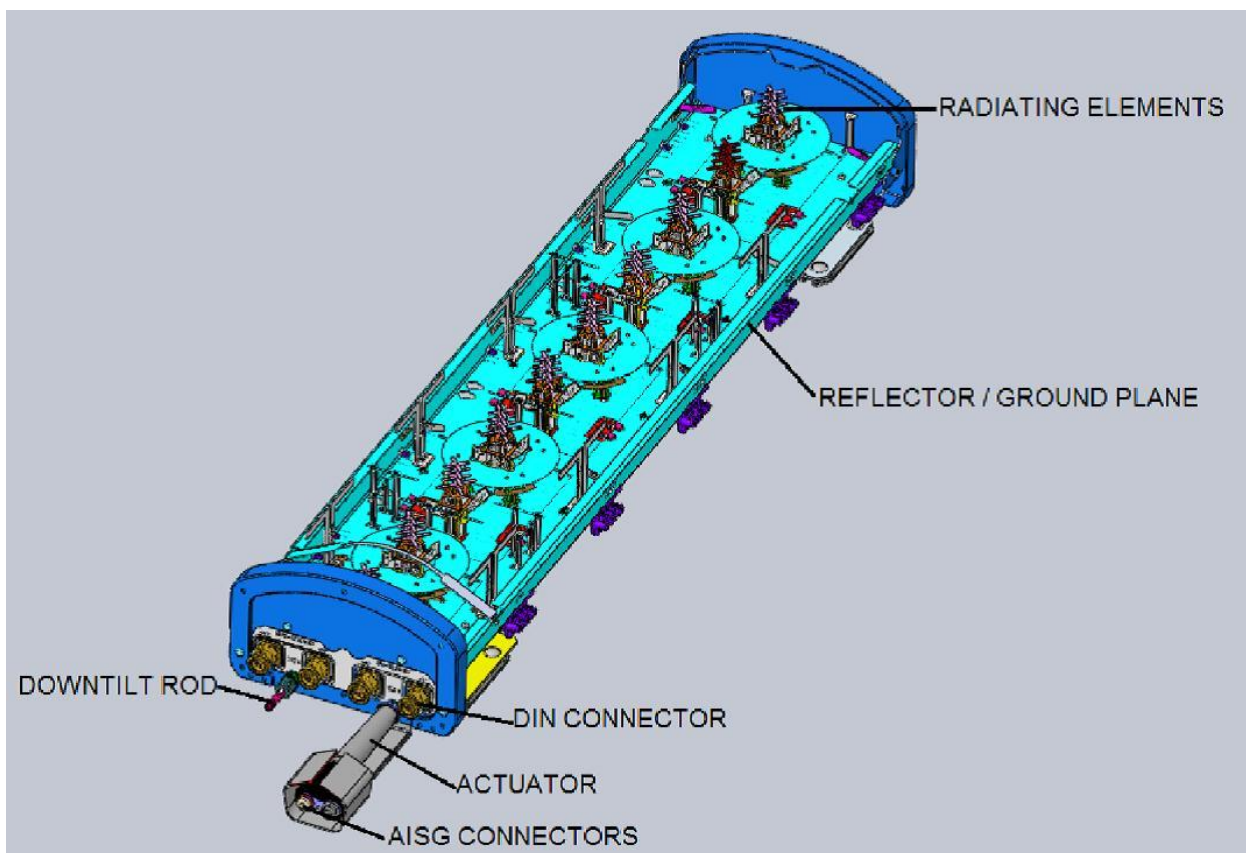


Figure 1 – Internals of a typical modern antenna structure for mobile wireless applications. This has four electrical ports.

We see in this structure a total of 18 radiating antenna elements; 5 high band with a polarization of +45° and five with a polarization of -45°, along with 4 low band of each polarization. When packaged in a common radome we refer to this overall structure as a single antenna even though there are 18

¹ Coaxial RF connectors standardized by the Deutsches Institut für Normung (DIN).

antenna elements inside. We refer to this as a single cross polarized column with two frequency bands interspersed. Also, even though the tilt actuator is motorized, we refer to this as a passive antenna because there are no active elements in the signal paths. (Active electronics use DC power to amplify or transform signals.) The 2012 white paper released by 4G Americas provides a detailed description of Active Antennas (AA) that include the radio transceivers inside the radome as well. Generally, the taller an antenna is, and the more elements there are in a column, the more resolution we have in shaping the vertical characteristics of the radiated pattern. That is to say, doubling the height allows us to about halve the vertical beam width and about double the antenna gain. This is tied to the wavelength so as the frequency doubles with a fixed height radome, we also tend to be able to double the antenna gain and halve the vertical beam width.

Consequently, in many installations where the antennas are limited to a fixed height such as 6 feet for esthetic and zoning reasons, we see that the higher frequency bands can have twice the antenna gain (3dB) as the lower frequency bands.

Likewise, the antenna width impacts the horizontal beam width. This is why a six sectored installation requires antennas that are about double the width of three sectored installations.

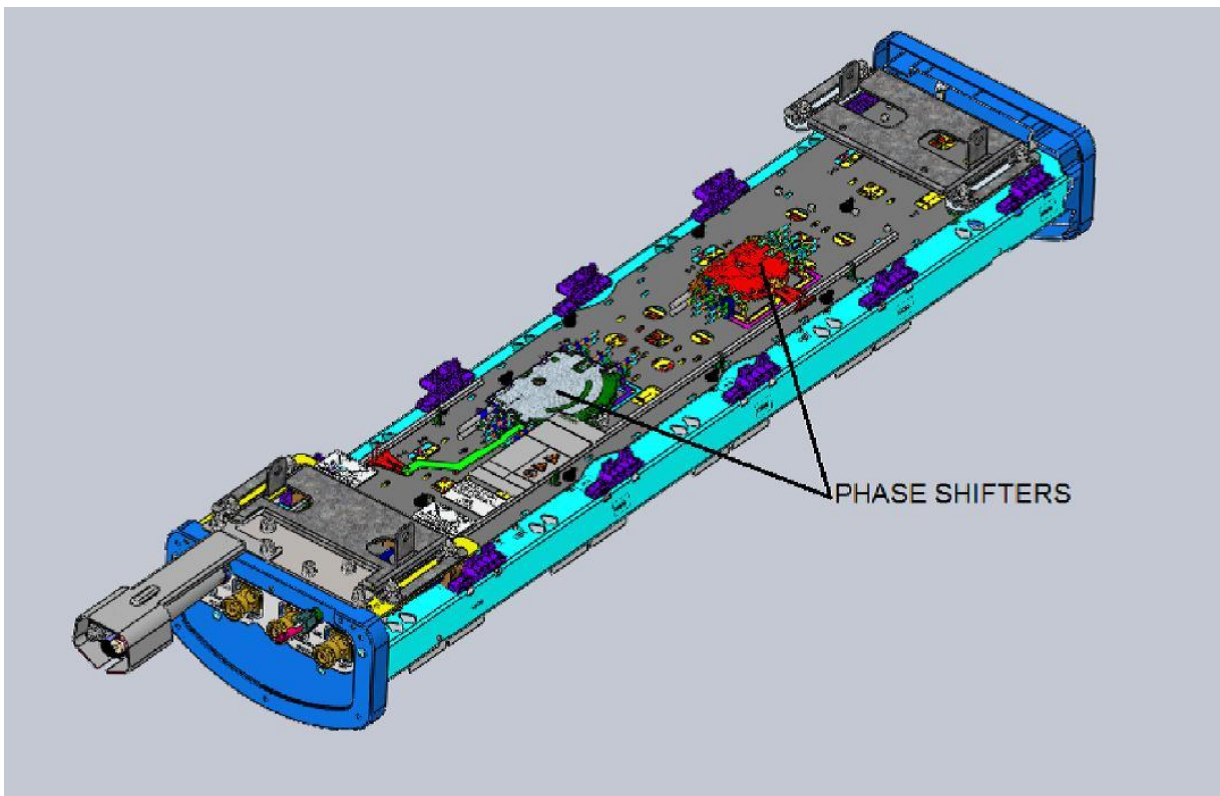


Figure 2 – View of the back of a typical modern antenna showing the tilt mechanisms.

More detailed definitions and acronyms concerning antennas are listed in the Appendix. In addition, definitions of base station antenna parameters and associated and standards recommendations can be found in a Next Generation Mobile Network (NGMN) Alliance whitepaper entitled “NGMN

Recommendations on Base Station Antenna Standards”.² This paper addresses the base station antennas typically used in FDD systems and in some TDD systems. A second NGMN whitepaper covers the advances in multi-column beamforming antenna that are being used in TDD systems. It is entitled, “Multi-Antenna Technology – Multi-Antenna Future Requirements”.³

Base station antenna technology has progressed in response to industry requirements and trends. The key drivers have been the continuing addition of cellular frequency bands, the integration of more functionality into single radome housing, and antenna techniques that contribute additional capacity to cellular networks.

² NGMN, Recommendations on Base Station Antenna Standards, version 9.6, 15 Jan 2013 URL:
<http://www.ngmn.org/nc/downloads/techdownloads.html>

³ NGMN, Multi-Antenna Technology – Multi-Antenna Future Requirements, version 2.3, 6 Feb 2013 URL:
<http://www.ngmn.org/nc/downloads/techdownloads.html>

2. MIMO WITH LTE

For many years base station antennas have been modified in one way or another to optimize the transmission or reception of signals. Multiple antenna elements may be used to shape beams and steer nulls in one direction or another. In the terminal, too, one may double the number of receive antennas to nearly double the received power and increase the SINR by nearly 3 dB.

However, if we add antenna elements at both the base station and at the terminal, then we are able to introduce an important new capability of using multiple antennas to input signals into space and multiple antennas to output the signals. This is referred to as Multiple Input and Multiple Output (MIMO). MIMO schemes are characterized by the number of antennas transmitting into the air, M , and the number of antennas receiving those same signals at the receiver(s), N ; designated as “ $M \times N$.” So, for example, the downlink may use, for example, 4 transmit antennas at the base station, and two receive antennas in the terminal, which is referred to as “4x2 MIMO.” The uplink might use one single transmit antenna in the terminal and 4 receive antennas at the base station, for “1x4 SIMO” operation. The “ $M \times N$ ” refers to the number of antennas in each end of the link (downlink or uplink) and not to the number of antennas at just one end of the link. As another typical example, an operator uses 2 transmit antennas and 4 receive antennas in the base stations while the terminal uses two receive antennas and one transmit antenna, so the downlink is 2x2 MIMO and the uplink is 1x4 SIMO. The base station is said to have 2T4R and the terminal, 1T2R.

The multiple antennas at the terminal side may all be within a single user’s terminal in which case we refer to this as Single User MIMO, or “SU-MIMO.” If channel conditions are good, this single user may receive multiple streams of data, nearly multiplying the obtainable peak throughput by the number of antennas. Alternatively, Multi-User MIMO or “MU-MIMO” refers to having multiple streams destined for multiple users, multiplying the aggregate cell throughput by the number of antennas.

What constitutes an antenna? Two metal wires connected to an RF transmit or receive chain may form two antennas, but if they are wrapped around each other or otherwise too close together, their signals will be highly correlated and won’t produce distinguishable signals at the other end of the link. If the two wires are very far apart, say several km, then their coherence is challenged and it is likely that one or the other will always be received weakly at the other end of the link. A happy medium exists when two antennas are very close together but cross polarized, then their signals are both coherent and reasonably de-correlated. We see here that the nature of the channel, how much multi-path or clutter it has, as well as the physical structure of the antennas – their spacing and polarization – all affect the quality of the MIMO configuration. Different antennas perform better in certain environments, and different signaling schemes (Transmission Modes or TMs) are appropriate for different antenna configurations and channels.

With the E-UTRAN (LTE) 3GPP specifications, an extremely sophisticated suite of transmission modes was defined for taking advantage of a wide variety of MIMO antenna and channel situations. With LTE-Advanced, there are 10 different Transmission Modes (TMs) applicable to 1, 2, 4, or 8 base station transmit antennas and 2, 4 or 8 terminal receive antennas. The base station’s scheduler dynamically adapts the modes to adjust the number of streams as the rank of the channel changes with time, and the terminals may be requested to signal back channel state information; or open loop transmit diversity can be used if spatial multiplexing is less effective. The rank refers to how many separate signal paths can be recognized by the receiver. Mathematically, this corresponds to the rank of the matrix representing the connectivity of the input to the output antennas – the number of independent paths. If all antennas are co-polarized, in free space or in an anechoic chamber where

there are no reflections, the rank collapses to 1 and no MIMO gains can be had, except for the added power received from multiple antennas. Polarization diversity increases the rank to the extent to which the channel sustains the independence of the signals transmitted on separate polarizations. Thus, a cross-polarized transmission pair in the same anechoic chamber can communicate with a cross-polarized pair of receive antennas with a rank of 2. We say that the channel is rich in multipath when the rank is high. Mathematically, the rank is limited to the minimum of the number of rows and columns corresponding to the lesser of the number of transmit and receive antennas. Therefore, a 4x2 MIMO system can have a rank of no more than 2, and we can transmit no more than 2 streams to that receive terminal.

We recognize that currently hand held terminals are limited by power and cost to having a single transmit antenna (at least for a particular carrier frequency) limiting uplink to 1xN SIMO, consequently we focus on the downlink MIMO operation.

2.1 LTE DOWNLINK MIMO BASICS

Figure 3 below shows the taxonomy of antenna configurations supported in Release-10 of the LTE standard (as described in 3GPP Technical Specification TS 36.211, 36.300). The LTE standard supports 1, 2, 4 or 8 base station transmit antennas and 2, 4 or 8 receive antennas in the User Equipment (UE), designated as: 1x2, 1x4, 1x8, 2x2, 2x4, 2x8, 4x2, 4x4, 4x8, and 8x2, 8x4, and 8x8 MIMO, where the first digit is the number of antennas per sector in the transmitter and the second number is the number of antennas in the receiver. The cases where the base station transmits from a single antenna or a single dedicated beam are shown in the left of the figure. The most commonly used MIMO Transmission Mode (TM4) is in the lower right corner, Closed Loop Spatial Multiplexing (CLSM), when multiple streams can be transmitted in a channel with rank 2 or more.

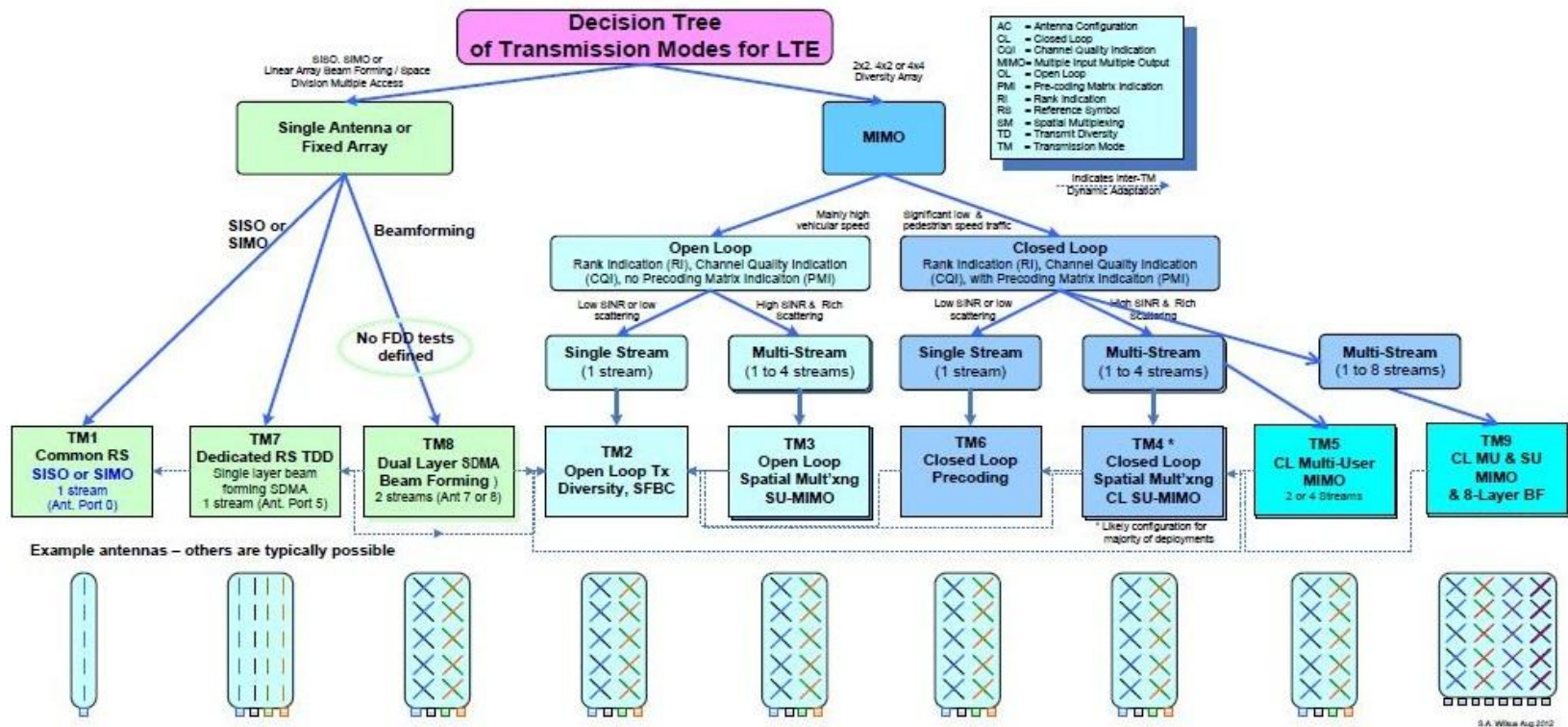


Figure 3 – Taxonomy of smart antenna processing algorithms in LTE Release 10. Shadows behind blocks indicate that they are capable of transmitting multiple streams. (LTE Release 11 recently added Transmit Mode 10 with explicit support for CoMP (Coordinated MultiPoint Transmission Reception) use which is not shown.)

These transmission modes are implemented through physical antennas described further in Figure 7 later in the section.

Beyond the single antenna or beamforming array cases diagrammed above, the LTE standard supports Multiple Input Multiple Output (MIMO) antenna configurations as shown on the right of Figure 3. This includes Single User (SU-MIMO) protocols using either open loop or closed loop modes as well as transmit diversity and Multi-User MIMO (MU-MIMO). In the closed loop MIMO mode, the terminals provide channel feedback to the eNodeB with Channel Quality Information (CQI), Rank Indications (RI) and Precoder Matrix Indications (PMI). These mechanisms enable channel state information at the transmitter which improves the peak data rates, and is the most commonly used scheme in current deployments. However, this scheme provides the best performance only when the channel information is accurate and when there is a rich multi-path environment. Thus, closed loop MIMO is most appropriate in low mobility environments such as with fixed terminals or at pedestrian speeds.

In the case of high vehicular speeds, Open Loop MIMO may be used, but because the channel state information is not timely, the PMI is not considered reliable and is typically not used. In TDD networks, the channel is reciprocal and thus the DL channel can be more accurately known based on the uplink transmissions from the terminal (the forward link's multipath channel signature is the same as the reverse link's – both paths use the same frequency block). Thus, MIMO improves TDD networks under wider channel conditions than in FDD networks.

One may visualize spatial multiplexing MIMO operation as subtracting the strongest received stream from the total received signal so that the next strongest signal can be decoded and then the next strongest, somewhat like a multi-user detection scheme. However, to solve these simultaneous equations for multiple unknowns, the MIMO algorithms must have relatively large Signal to Interference plus Noise ratios (SINR), say 15 dB or better. With many users active in a base station's coverage area, and multiple base stations contributing interference to adjacent cells, the SINR is often in the realm of a few dB. This is particularly true for frequency reuse 1 systems, where only users very close to the cell site experience SINRs high enough to benefit from spatial multiplexing SU-MIMO. Consequently, SU-MIMO works to serve the single user (or few users) very well, and is primarily used to increase the peak data rates rather than the median data rate in a network operating at full capacity.

Angle of Arrival (AoA) beamforming schemes form beams which work well when the base station is clearly above the clutter and when the angular spread of the arrival is small, corresponding to users that are well localized in the field of view of the sector; in rural areas, for example. To form a beam, one uses co-polarized antenna elements spaced rather closely together, typically $\lambda/2$, while the spatial diversity required of MIMO requires either cross-polarized antenna columns or columns that are relatively far apart. Path diversity will couple more when the antennas columns are farther apart, often about 10 wavelengths (1.5m or 5' at 2 GHz). That is why most 2G and 3G tower sites have two receive antennas located at far ends of the sector's platform, as seen in the photo to the right. The signals to be transmitted are multiplied by complex-valued precoding weights from standardized codebooks to form the antenna patterns with their beam-like main lobes and their nulls that can be directed toward sources of interference. The beamforming can be created, for example, by the UE PMI feedback pointing out the preferred precoder (fixed beam) to use when operating in the closed loop MIMO mode TM4.



LTE (4G) provides several different variations for Multiple Input Multiple Output (MIMO) techniques, from beamforming, to MIMO, or single antenna schemes, through selection of one of 9 Transmission Modes (TMs). These Transmission Modes (TMs) classified above in Figure 3 are detailed further in the table below. This table includes TM8, which is introduced in LTE Release 9 to support dual layer beamforming (Multi-User MIMO), and TM9 which is introduced in Release 10 (LTE-Advanced) to increase the number of layers from 4 to 8. The antenna types refer to those diagrammed in Figure 6.

Table 1 – eNodeB Transmission Modes in of the LTE standard through Release 10.

TM	Title	Antenna Type	Description
1	Single Transmit Antenna Port 0 SIMO, rank 1	1 column (A) or Other antenna types with Tx only on 1 column	This TM uses no spatial multiplexing. It is useful for some single antenna femtocells and some control channels.
2	Open Loop Transmit Diversity For rank 1	2 or 4 antennas (D, E, F, H, I)	The default and most robust transmit mode where the same information is transmitted through multiple antennas, each with different coding/frequency resources. Alamouti codes are used with 2 antennas as the Space Frequency Block Codes (SFBC). For 4TX, SFBC along with Frequency Shift Time Diversity (FSTD) are used. This is a common fallback mode with dynamic adaptation from other MIMO and beamforming modes. It has no dynamic rank adaptation but can adapt the link through CQI, i.e. dynamic adaptation.

<p>3</p>	<p>Open Loop Spatial Multiplexing SU-MIMO with Cyclic Delay Diversity, CDD</p> <p>Multi-Stream</p> <p>For ranks 2 to 4</p>	<p>2 or 4 antennas (B, D, E, F, H, I)</p>	<p>As an open loop mode, this requires no PMI, but utilizes RI (rank adaptation) and CQI information from the UE for adaptation on a TTI (Transmission Time Interval) level, and is supporting multi-stream use for channels that are rapidly changing such as with high velocity UEs to harvest diversity and spatial multiplexing benefits.</p> <p>Precoding of 2x2 MIMO uses the following table as defined in 3GPP TS 36-211 Table 6.3.4.2.3-1.</p> <table border="1" data-bbox="618 506 1432 1041"> <thead> <tr> <th>Code Book</th> <th>1 Layer</th> <th>2 Layers</th> </tr> </thead> <tbody> <tr> <td>0</td> <td>$\frac{1}{\sqrt{2}} \begin{pmatrix} 1 \\ 1 \end{pmatrix}$</td> <td>$\frac{1}{\sqrt{2}} \begin{pmatrix} 1 & 0 \\ 0 & 1 \end{pmatrix}$</td> </tr> <tr> <td>1</td> <td>$\frac{1}{\sqrt{2}} \begin{pmatrix} 1 \\ -1 \end{pmatrix}$</td> <td>$\frac{1}{\sqrt{2}} \begin{pmatrix} 1 & 1 \\ 1 & -1 \end{pmatrix}$</td> </tr> <tr> <td>2</td> <td>$\frac{1}{\sqrt{2}} \begin{pmatrix} 1 \\ i \end{pmatrix}$</td> <td>$\frac{1}{\sqrt{2}} \begin{pmatrix} 1 & 0 \\ i & -i \end{pmatrix}$</td> </tr> <tr> <td>3</td> <td>$\frac{1}{\sqrt{2}} \begin{pmatrix} 1 \\ -i \end{pmatrix}$</td> <td>Not Applicable</td> </tr> </tbody> </table> <p>The antenna patterns arising from these codebook entries are shown in Figure 4. The Cyclic Delay Diversity (CDD) creates additional time diversity.</p>	Code Book	1 Layer	2 Layers	0	$\frac{1}{\sqrt{2}} \begin{pmatrix} 1 \\ 1 \end{pmatrix}$	$\frac{1}{\sqrt{2}} \begin{pmatrix} 1 & 0 \\ 0 & 1 \end{pmatrix}$	1	$\frac{1}{\sqrt{2}} \begin{pmatrix} 1 \\ -1 \end{pmatrix}$	$\frac{1}{\sqrt{2}} \begin{pmatrix} 1 & 1 \\ 1 & -1 \end{pmatrix}$	2	$\frac{1}{\sqrt{2}} \begin{pmatrix} 1 \\ i \end{pmatrix}$	$\frac{1}{\sqrt{2}} \begin{pmatrix} 1 & 0 \\ i & -i \end{pmatrix}$	3	$\frac{1}{\sqrt{2}} \begin{pmatrix} 1 \\ -i \end{pmatrix}$	Not Applicable
Code Book	1 Layer	2 Layers																
0	$\frac{1}{\sqrt{2}} \begin{pmatrix} 1 \\ 1 \end{pmatrix}$	$\frac{1}{\sqrt{2}} \begin{pmatrix} 1 & 0 \\ 0 & 1 \end{pmatrix}$																
1	$\frac{1}{\sqrt{2}} \begin{pmatrix} 1 \\ -1 \end{pmatrix}$	$\frac{1}{\sqrt{2}} \begin{pmatrix} 1 & 1 \\ 1 & -1 \end{pmatrix}$																
2	$\frac{1}{\sqrt{2}} \begin{pmatrix} 1 \\ i \end{pmatrix}$	$\frac{1}{\sqrt{2}} \begin{pmatrix} 1 & 0 \\ i & -i \end{pmatrix}$																
3	$\frac{1}{\sqrt{2}} \begin{pmatrix} 1 \\ -i \end{pmatrix}$	Not Applicable																
<p>4</p>	<p>Closed Loop Spatial Multiplexing SU-MIMO</p> <p>Multi-Stream</p> <p>For rank 2 to 4</p>	<p>2 or 4 antennas (B, D, E, F, H, I)</p>	<p>To allow the UE to estimate the channels needed to decode multiple streams, the eNodeB transmits Reference Signals (RS) on prescribed Resource Elements, the CRS (Cell-specific Reference Symbols) per antenna. The UE replies with the Precoding Matrix Indicator (PMI) indicating which precoding is preferred from the codebook given above for TM3, adding beamforming benefits. The CRS is applied for UE demodulation channel estimation for TM1 through TM6.</p>															
<p>5</p>	<p>Closed-Loop Multi-User MIMO</p> <p>For rank 2 to 4</p>	<p>2 or 4 antennas (B, C, E, F, H)</p>	<p>Similar to TM4 but for the multi-user case.</p> <p>This is a basic MU-MIMO scheme from Release 8, and is not widely used.ⁱ</p>															

6	<p>Closed Loop Rank 1 Precoding</p> <p>For rank 1 Spatial Multiplexing</p>	<p>2 or 4 antennas</p> <p>(D, E, F, G, H, I)</p>	<p>For a single layer (rank 1) channel, this mode uses PMI feedback from the UE to select the preferred (one layer) codebook entry from the codebook given in TM3 above.</p> <p>Precoding the signal at the baseband for the different antennas results in the beamforming shown below in Figure 4.</p> <p>This precoding beamforming selected by UE PMI feedback is not cognizant of multi-user intercell interference and is somewhat distinct from the classical beamforming based upon Angle of Arrival or similar approaches used in TM7 and TM8.</p>
7	<p>Single Layer Beamforming (angle of arrival) for port 0</p> <p>Linear Array Beamforming Antenna port 5</p>	<p>Virtual Antenna port 5 made from (B, C, E, G)</p>	<p>In this mode, both the data and an additional Demodulation Reference Signals (DMRS) are transmitted with the same UE-specific antenna weights which form a virtual antenna pattern (Antenna port 5) so that the UE does not distinguish the actual physical antennas as in the classical beamforming approach.</p> <p>The specific method of calibration and determining weights is left to implementations such as Angle of Arrival (AoA), MUSICⁱⁱ or ESPRITⁱⁱⁱ.</p> <p>TM7 support is mandatory for TD-LTE and optional for FDD-LTE.</p>
8	<p>Dual Layer Beamforming based upon angle of arrival</p> <p>SU-MIMO or MU-MIMO</p>	<p>Virtual antenna ports 7 and 8</p> <p>Made from (C, E, G)</p>	<p>Introduced in Release 9, TM8 does classical beamforming with UE specific DMRSs, like TM7, but for dual layers. This permits the eNodeB to weight two separate layers at the antennas so that beamforming can be combined with spatial multiplexing for one or more UEs.</p> <p>The two layers can be targeted to one or two UEs.</p> <p>Similar to TM7, TM8 support is mandatory for TD-LTE and optional for FDD-LTE. TM8 can also be used in vertical beamforming enabled by an Active Antenna System.</p>
9	<p>8 layer SU/MU-MIMO</p>	<p>Ports 7 to 14</p>	<p>Introduced in Release 10, as part of LTE-Advanced, TM9 implements 2, 4 or 8 virtual ports, It is the only TM suitable for 8 ports, and most suitable for MU-MIMO with dynamic switching from SU-MIMO. It is applicable to either TDD or FDD systems.</p>
10	<p>8 layer Transmission</p>	<p>Ports 7 to 14</p>	<p>Introduced in Release 11 as part of LTE-Advanced, TM10 is an enhancement to TM9 to explicitly support CoMP (Coordinated MultiPoint transmission reception) with improved interference measurements, antenna port co-location assumptions and multi-point CSI feedback. TM 10 also supports Multicast Broadcast Single Frequency Network (MBSFN).</p>

For transmit modes 3 through 6, a precoding type of beamforming is used to phase the signals on multiple antennas and to concentrate the antenna pattern toward various horizontal directions when transmitting to a UE on the downlink. The UE sends a feedback message on a TTI (Transmission Time Interval) level that recommends the precoder matrix that will optimize the quality of the link between the base station and the UE. For the case of two antenna columns, the precoding coefficients given in table entry TM3 yield the horizontal antenna gain patterns shown below in Figure 4. The two antenna columns are assumed to be separated by $\lambda/2$, with antenna type “B” - from Figure 6, and perfect antenna array calibration is assumed. Here we can see that codebook entry 1 would be appropriate for transmitting a UE located to the left or right of the antenna’s boresight. Note that codebook entry 1 provides less interference to UEs in other cells that are located in the antenna’s boresight. Codebook entry 2 would be best for a UE located to the right of the boresight. Codebook entry 2 will reduce interference into adjacent cells to the left of boresight, helping to improve the typical SINR for the network’s UEs.

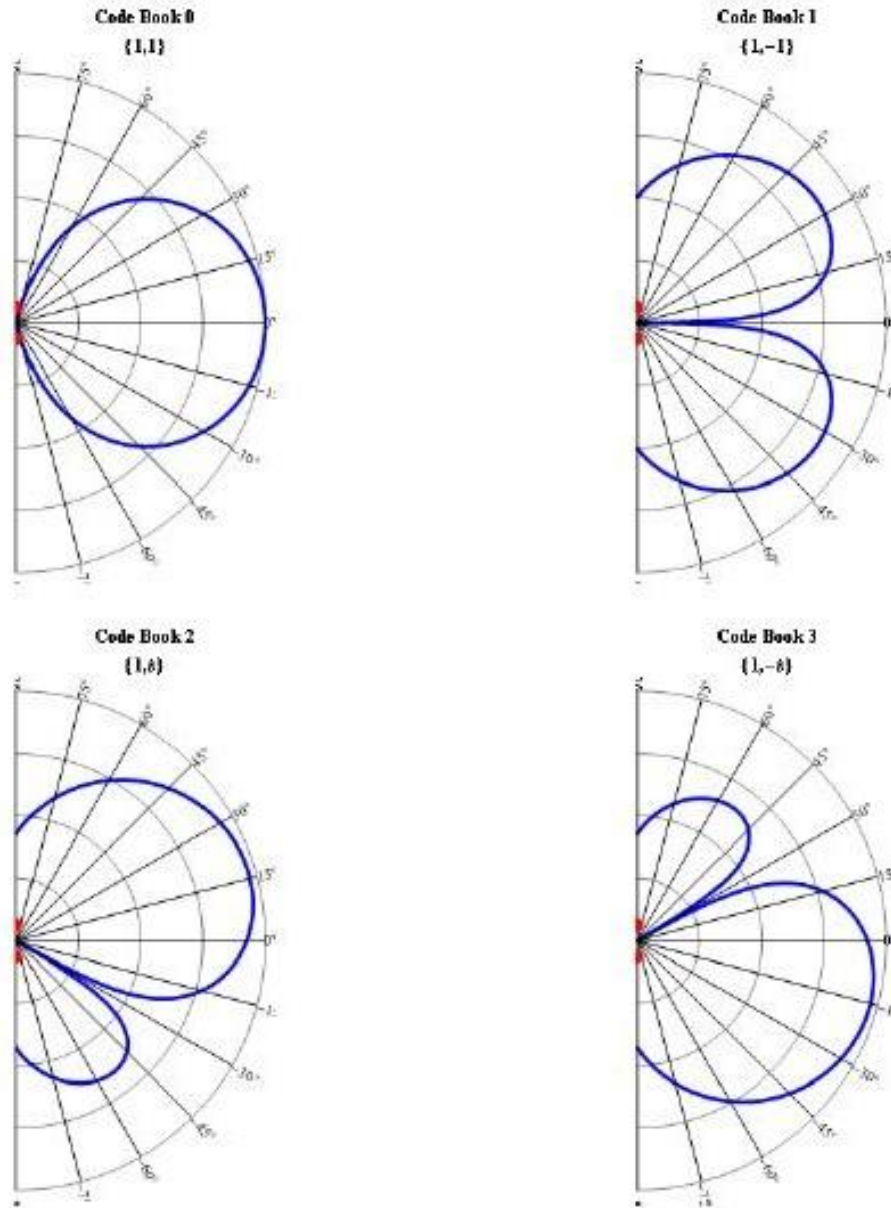


Figure 4 – Antenna patterns resulting from the two antenna codebook entries of TM3, TM4 and TM6. The views are horizontal cuts as seen from above with the two antennas spaced by half a wavelength and represented by the red dots. The element factor is taken from 3GPP TR 25.996. This assumes a spacing of $\lambda/2$ and perfect calibration.

A 4-antenna version of the above figure includes 16 different antenna patterns. They are generated by a linear array of 4 antenna columns such as in antenna style C in Figure 6. However, this antenna is not commonly used today because it is twice as wide as antenna type E which provides cross polarization diversity advantage.

For illustrative purposes, the general applicability of the various TM modes is shown below in Figure 5:

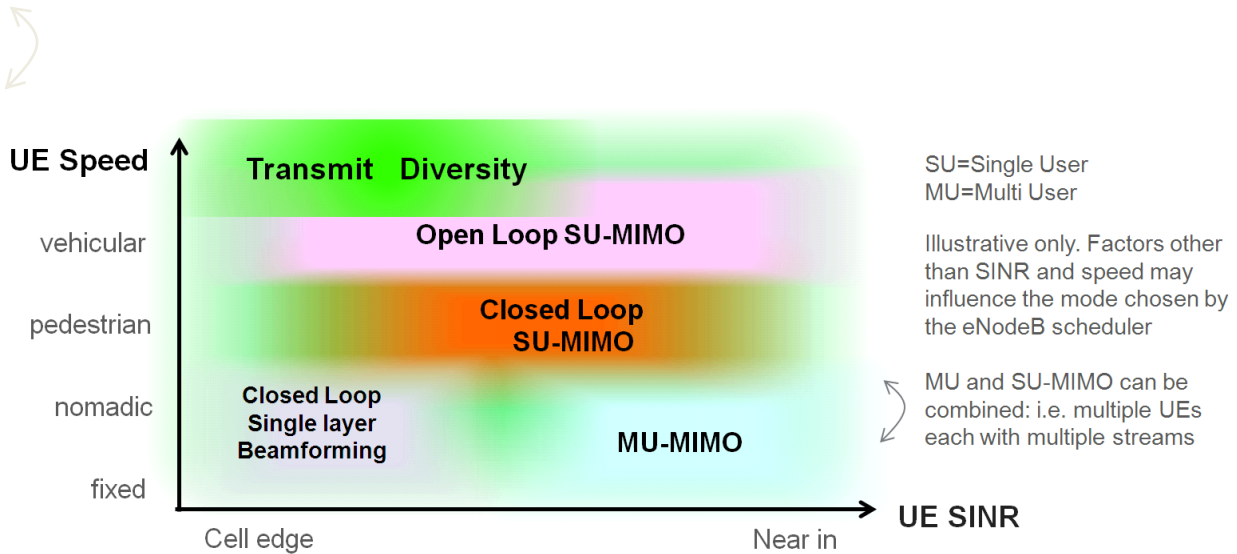


Figure 5 – MIMO TM Modes in LTE-Advanced selected on the basis of UE SINR and speed.

2.2 ANTENNA CONFIGURATIONS FOR MIMO

MIMO systems place requirements on the RF link as to be rich enough to make the channel separable to detect multiple streams, similar to the receive diversity system requirements that are in place for current cellular networks, that is, there must be de-correlation between the channels received at the antennas. This signal richness is provided by the environment with e.g. reflections and supported by space diversity achieved by the separation of the antennas, or by the use of polarization diversity when implemented by the use of orthogonal antenna elements.

Early cellular systems employed spatial diversity and typically used two vertically polarized antennas separated by a distance of 10 wavelengths, or greater, at the frequency of operation. Most cellular providers have switched to polarization diversity, utilizing cross polarized antennas, which have been shown to provide equivalent if not better diversity gain than it does for spatial diversity.^{iv} Dual polarized antennas have the added benefit of integrating two antenna arrays into one radome housing while maintaining the same size.

Most antenna properties, and their associated specifications, influence the illuminated coverage of the cell site topography and the link budget between the base station and handset. However, for dual-pol antennas, both cross-polar discrimination and port-to-port isolations can affect the diversity or MIMO performance of the system by introducing correlation between the channels. Studies have shown that the standard specifications that meet the requirements for effective receive diversity performance^v also provide adequate de-correlation for effective MIMO system performance.^{vi}

In summary, a standard dual polarized antenna (e.g. antenna D in Figure 6) works well for 2x2 MIMO, as do two spatially separated dual-pol antenna for 4x2 or 4x4 MIMO. A quad antenna, which packages two dual polarized arrays into one radome (e.g. antenna type E in Figure 6), provides effective 4x2, or 4x4 MIMO performance in a compact width radome.^{vi} With the two columns of cross-pol elements, the antenna can transmit on two cross polarized elements in the two columns, and receive on all 4 branches, or if 4 transmit RF chains are used, then 4x2 MIMO can be used in the downlink. Spatial separation of 1λ between dual-polarized arrays is the norm for quad antennas. Studies presented in this paper indicated that quad antennas that have a spatial separation of less than 1λ can provide throughput gains for closed-

loop, spatial multiplexing, pre-coded beamforming (LTE transmission mode TM4), albeit at the possible expense of degraded diversity performance and some compromise in antenna performance.

Physically, these antennas are categorized below in Figure 6 where the short lines correspond to individual antenna elements, typically arranged in columns. Such columns are able to define the vertical beam width required to properly illuminate a cell sector and which is a characteristic of base station antennas. Typically the antenna elements in each column are interconnected and share a common RF connector shown below the columns. These correspond to the individual RF cables that connect the radios and their amplifiers. The configurations shown are restricted to no more than 4 cables per sector, corresponding to the 4x4 limit in the Release 8/9 standards.

Trans. Mode	Antenna Config.	Figure	Description
TM1	1V	(A)	1 Column with vertical polarization (V-Pol)
TM5 TM7 (TDD)	ULA – 2V	(B)	2 Closely spaced V-pol columns
TM5 TM7-8 (TDD)	ULA-4V	(C)	4 V-pol columns
TM2-4, TM6	DIV 1X	(D)	1 Column with dual-slant-45 polarization (X-pol) for 2 branch MIMO
TM2-6 TM7-8 (TDD)	CLA-2X	(E)	2 Closely spaced X-pol columns (Quad Port) 4 branch MIMO or 2 antenna beamforming
TM2-6	CLA-3X	(F)	1 X-pol center column between two closely spaced x-pol columns. The outer columns have only one polarization active, the other two are shown in dashed lines suitable for use with another frequency band or for “padding”.
TM2-6 TM7-8 (TDD) M9 (w/o Butler matrix)	CLA-4X (aka BM-4X)	(G)	4 X-pol columns with dual Butler Matrix TM9 can use up to 8 ports without a Butler Matrix for 4 antenna beamforming The Butler matrix in antenna G is used to distribute phase and amplitude weighted contributions of the 4 RF connectors to the 8 columns to form 4 separate beams (two for each polarization, each half as narrow a beam width as antenna E).
TM2-6	DIV-2X	(H)	2 Widely spaced X-Polarized columns
TM2-4, TM6	TX-DIV	(I)	2 Widely spaced Vertically polarized columns

Figure 6 — Antenna configurations with the constraint of no more than 4 antenna cables per sector for a total of 12 cables for a 3 sector system. (ULA=Uniform Linear Array, DIV=Diversity, CLA=Clustered Linear Array) The color code for the RF Coaxial connectors is the same as for the elements, except for the Butler Matrix case. These illustrative diagrams represent a single band. Additional frequency bands may be overlaid within the radomes containing these antenna elements.

No one antenna configuration is optimal for all environments, for example, in rural areas where the eNodeB antennas are located above the clutter, antennas that can form beams such as C and G are best. In urban macrocellular environments where angle spread is large, cross-polarized antennas E, G, or H give best gains from polarization diversity. In urban microcellular base stations that are embedded in the clutter and the angle of arrival spread is large, then the antenna (H) is expected to be good at providing the greatest path diversity comparable downlink spectral efficiency.

2.2.1 TYPICAL 8 BRANCH CLUSTERED LINEAR ARRAY (CLA-4X) ANTENNA

As an example of a practical modern antenna, Figure 7 illustrates a typical dual polarized array with 4 columns of cross-dipole radiators, a calibration circuit, and 9 connectors. Generally, 1.5 VSWR is required on all antenna and calibration ports. Isolation between co-polarized and cross-polarized antenna ports is desired to be greater than 25 dB and 30 dB respectively.

This antenna can be used in either broadcast mode or beamforming mode. In broadcast mode, a typical 65° azimuth beam width is required for a tri-sector system with approximately 17 dBi gain. In beamforming mode, a 4-column array can provide an additional 6 dB antenna gain at boresight reducing to about 3 dB additional gain at the maximum scan angle of $\pm 60^\circ$. For MIMO applications, cross-polarization rejection between the orthogonal +45/-45 polarized ports of 20 dB at boresight and 10 dB over sector ($\pm 60^\circ$) is typically required.

A broadband multicolumn antenna with Remote Electrical Tilt (RET) would need to have similar elevation pattern performance of a fixed tilt antenna over a downtilt range of typically 0°-10°. To reduce adjacent cell interference, typically 16 dB upper sidelobe suppression is required.

For beamforming accuracy, a calibration circuit is required to reduce effects of transceiver variations between paths. The passive calibration circuit typically requires amplitude balance between paths of < 0.7 dB and phase balance of < 5°.

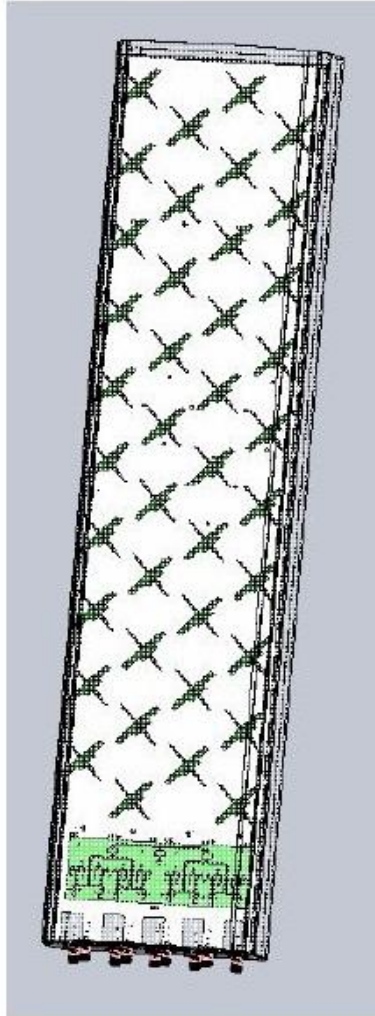


Figure 7 – Typical 4 column dual polarized beamforming antenna (source: Commscope). This antenna radome has 8 separate coaxial connectors, suitable for 8T8R operation common with high band TDD systems such as TD-SCDMA and TD-LTE.

2.2.2 MULTI-BEAM ANTENNAS

Multi-beam antennas are starting to be used in cellular networks where it is desired to increase capacity of existing cells. A single sector antenna can be replaced by two or more cell sectors, e.g. cell-split by higher order of sectorization. For this it is convenient to replace the single sector antenna with an antenna providing two or more beams in the horizontal plane.

Another application is where an area with extremely high traffic density must be served from a single point. This frequently arises in the context of stadiums or open-air venues such as music concerts or sports events. Here, different sectors of the crowd are covered by separate narrow beams. Because music events and the like are often one-time or annual events, there is growing interest in high capacity COW (cell-on-wheels) systems with multi-beam antennas providing horizontally sectorized multiple cell coverage that can be moved in to cover the particular event. A typical panel antenna for covering such a crowd is a cross polarized 9 column antenna (2x9 ports) to produce 9 sectors with dual branch receive, as shown below in Figure 8. The left figure is for an array of 10x6 elements driven from a Butler matrix

with 5 inputs forming the five beams shown and the right figure is from an array of 20x6 elements used to form 9 cross polarized beams.

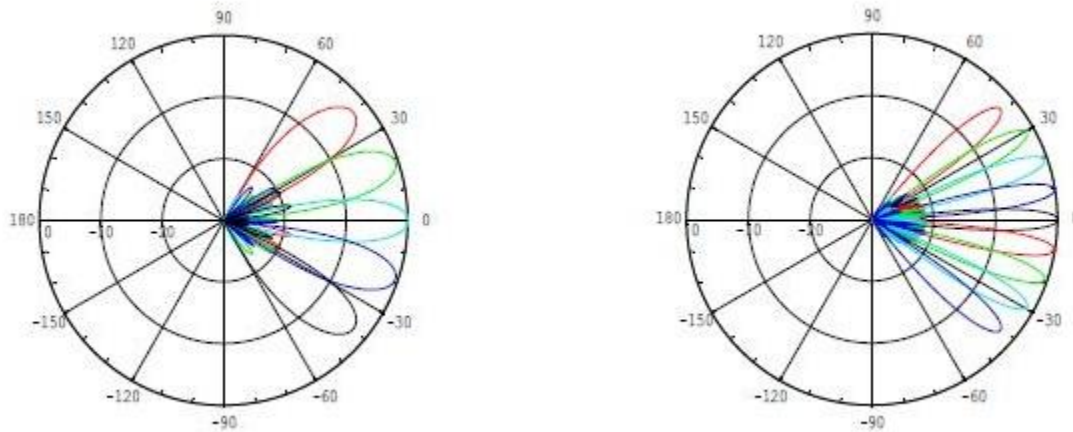


Figure 8 – Multi-beam transmit patterns. The left figure corresponding to an antenna array with a center beam gain of 20.5 dBi; the right figure has a center beam gain of 23 dBi.

The technology seems to have application for capacity enhancement in many situations. Another example tilts the two polarizations separately tilted to produce two rows of 9 beams as shown in Figure 9. This product is touted for covering tiers of bleachers in sports stadiums.

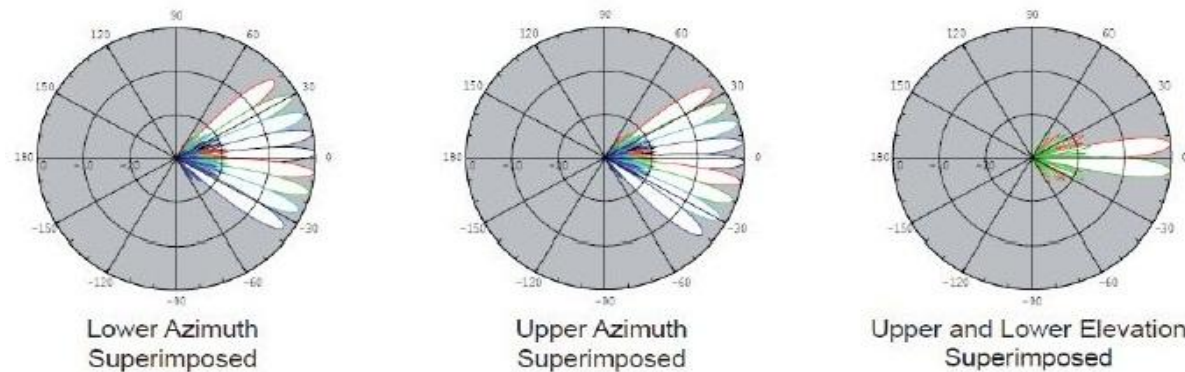


Figure 9 – Multi-Beam Antenna array pattern for 2 rows of 9 beams.^{vii}

Two-beam antennas have been implemented as RET antennas with the networks implemented in each row of the array. This is also possible with multi-beam antennas; however the complexity rapidly grows with the number of beams.

The basic antenna consists of an array of dual-polarization columns fed from two butler matrices so as to obtain a number of beams pointing at different azimuth angles.

A butler matrix is a microwave network with n input ports and n output ports allowing the forming of up to n beams when connected to the n port antenna. The input ports are all matched and isolated from each other as are the output ports. The network has the special characteristic that if a signal is applied to input

port i ($i=1, \dots, n$) then the output j ($j=1, \dots, n$) has phase $360(j-1)(i-1)/n$ degrees, which means that feeding element i radiates a beam at azimuth of $\sin^{-1}[\lambda/s*(i-1)/n]$ where s is the spacing of the columns.

2.3 PERFORMANCE OF THE VARIOUS ANTENNA CONFIGURATIONS

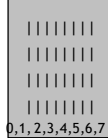
Of all the various antenna configurations illustrated in Figure 6 and the various transmission modes shown in Figure 3, which combinations should actually be used? How should we select the best ones? ^{viii}

The important metrics we consider in choosing between the various configurations are (1) spectrum efficiency under full load (full buffers) and (2) throughput of cell edge or cell border UEs – typically taken as the 5-percentile UE throughput. These metrics apply in both downlink and uplink scenarios. Simulations such as these help provide some comparisons among schemes, and even though the performance numbers are averages across several different environmental parameters, the actual field performance may differ considerably from one instance to another.

We chose between various numbers of downlink antenna columns for downlink Nx2 MIMO channels as shown below in Figure 10.^{ix} Here we see a summary of comparable simulations of Nx2 downlink performance of SU-MIMO performance in terms of Spectral Efficiency (SE) and Cell Border ThroughPut (CBTP) (taken as the 5 percentile throughput). These simulations were conducted assuming a FDD-LTE system operating with a 10 MHz carrier bandwidth at 2100 MHz. The simulation modeled TM4 (Closed Loop Spatial Multiplexing) for 2 and 4 branch transmissions, and TM9 for 8 branch transmissions.⁴ The particular numbers should not be the focus here but rather the relative performance of various antenna types. Here we see, for example, that CLA-2X with twice the number of antenna elements as DIV-1X provides about 20% aggregate increase over DIV-1X (aka CLA-1X), and a 32% increase in cell edge throughput. An additional doubling of columns to CLA-4X provides a similar percentage increase in performance (from 20% to 40% in aggregate throughput and 32% to 70% for cell edge throughput).

⁴ In addition, the simulations detailed here and in Figure 11 assume ideal calibration (zero phase difference) of transmit chains through to the antenna elements, vertically oriented UEs with vertically oriented antennas, and an average of case 1, and 3, UMi, UMa, RMa configurations given by 3GPP 36.814. A 21 cell scenario with a hexagonal grid of 7 sites is simulated as per ITU guidelines. The calculated SINR is used for dropping decisions, MCS selection corresponding to an Ideal Link Adaptation (LA) assumption. Full buffer traffic loads were assumed for 10 users per cell. Overheads and performance are based on 3GPP 36.814 assumptions..

Comparing Nx2 DL SU-MIMO – Closely Spaced BS Antennas

	1V	ULA-2V	DIV-1X	ULA-4V	CLA-2X	ULA-8V	CLA-4X
N x 2 SU-DL MIMO Configuration						 0,1,2,3,4,5,6,7	 0,4 1,5 2,6 3,7
SE CBTP [bps/Hz kbps]	1.7 470	2.0 620	1.9 540	2.4 830	2.3 710	2.8 1000	2.7 920
Gain vs reference % %	-12 -13	4 15	0 0 reference	26 53	20 32	43 85	40 70

Martin Schipporeit, Feb. 2013

Figure 10 – Downlink performance estimates for various closely spaced antenna configurations based upon simulations in multiple deployment scenarios (base station separations, down tilts, urban and rural, etc. 2100 MHz carrier frequency with a bandwidth of 10 MHz FDD. SE refers to spectral efficiency and CBTP the Cell Border Throughput.

We see, that the downlink performance of ULA configurations are slightly better than for CLA, an artifact of the simulation simplification of consistent vertical orientation of the handsets in the model. The aggregate throughputs are higher (though only slightly so) for, say ULA-2V than for DIV-1X, and ULA-8V vs. CLA-4X, but the cell edge performance is better by 15% or more. This can be anticipated by the ability of ULA schemes to form narrower beams (about half as narrow for the equivalent CLA antenna) that are more directed to the individual UE without adding as much intercell interference. What the ULAs give up in polarization diversity, they more than make up for in added antenna gain. Even so, these numbers should be interpreted with some humility as the model may not properly characterize the polarization diversity of the handsets and the polarization mixing of the real channels. The UE terminal antennas were modeled as co-polarized vertically, and of equal gain, for example. This is not generally the case for real-world terminals.

These observations are not recommendations. In addition, these results should be weighed against uplink performance and other aesthetic and practical considerations such as lease agreements which tend to cost more for wider antenna radomes.

With 10 wavelength separations modeled as “widely spaced” antennas, the following simulation results indicate that closely spaced columns are preferred for all vertical and crossed polarized antenna columns, just as we saw in Figure 11 above.

Comparing Nx2 DL SU-MIMO – Widely Spaced BS Antennas

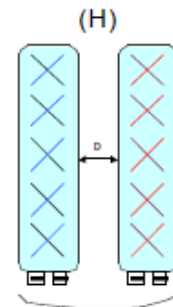
	1V	DIV-2V	DIV-1X	DIV-4V	DIV-2X	DIV-8V	DIV-4X
N x 2 SU-DL MIMO Configuration							
SE/CBTP [bps/Hz kbps]	1.7 470	2.0 540	1.9 540	2.2 650	2.2 640	2.3 700	2.2 710
Gain vs reference % %	-12 -13	2 1	0 0 reference	15 21	13 18	16 31	15 31

Martin Schipporeit, Feb. 2013

Figure 11 – Simulated downlink performance for various widely spaced antenna configurations. As in Figure 10, SE refers to the aggregate Spectral Efficiency and CBTP corresponds to the Cell Border (5 percentile) Through Put, (a/k/a the cell edge bit rate). As before, “mileage may vary” in actual field instances, so these numbers should be interpreted as comparisons only and not for absolute performance expectations.

2.4 AN ANALYSIS OF ANTENNA CONFIGURATIONS FOR 4X2 AND 4X4 MIMO

An attractive base station antenna solution for LTE supporting up to four layers in the downlink is to use two horizontally separated dual-polarized antennas such as shown to the right. This enables a compact antenna design that can utilize both the spatial and polarization dimensions. The amount of separation between the two antennas will have different impacts on the potential gains of beamforming, diversity, and spatial multiplexing. Realizing these gains puts conflicting demands on the antenna separation and different choices of antenna separation will result in different system performance profiles. The antenna size is also an important parameter from a site installation point of view. It influences various aspects, e.g., visual footprint, wind load, and site rental cost.



Results from a study on the impact of antenna separation on LTE system performance are presented.^x By means of system simulations, evaluations are performed to aid the understanding of the antenna separation trade-off. In addition, empirical support to the simulation results is provided by means of comparison to results from a measurement campaign.^{xi}

The simulations were performed with a detailed dynamic system simulator that includes models of adaptive coding and modulation, UE mobility, and delays in channel quality reports. It also contains an implementation of the 3GPP spatial channel model (SCM)^{xii} and the mutual information based link-to-system interface.^{xiii}

A simulation scenario similar to the defined 3GPP case 1^{xiv} was evaluated for different configurations with dual-polarized antennas at the BS using the closed loop spatial multiplexing transmission mode (transmission mode 4). 3GPP case 1 refers to a macro-cell reference system deployment type with the 3GPP SCM used for channel modeling. The network consisted of 19 sites separated 500 m with 3 cells per site and an average traffic load of 4 UEs per cell. Each antenna port of the BS antenna was modeled according to the BS antenna model^{xiii} regardless of antenna separation. The notation “ $m_{tx} \times n_{rx}$ ” will be used for an antenna configuration with m_{tx} transmit and n_{rx} receive antenna elements. Downlink (DL), 4x4, 4x2, and 2x2 configurations comprising one or two dual-polarized antennas at the UE and BS are investigated. For uplink (UL), 1x4 and 1x2 configurations comprising one vertically polarized antenna at the UE and one or two dual-polarized antennas at the BS (the E-UTRA standard for LTE assumes the use of at least two antennas in the UE, at least as a baseline).^{xv} Wideband PMI and frequency selective CQI was assumed in the simulations.

Next, we consider the performance impact of changing the separation, D , of two columns of base station antennas, such as the DIVERSity with two cross polarized (DIV-2X) type (H) in the figure above.

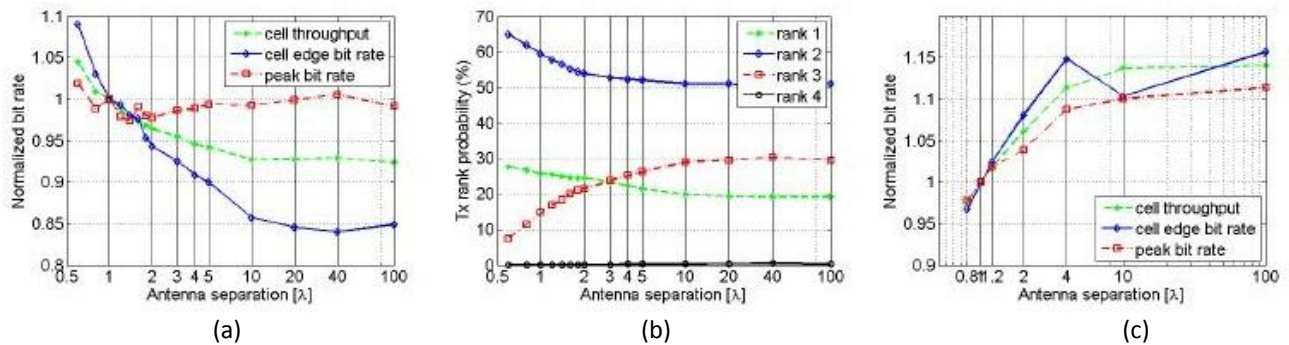


Figure 12 – Downlink bit rate (a), downlink transmission rank probability (b), and uplink bit rate (c) as a function of the two dual BS antennas separation for the 4x4 and 1x4 antenna configuration in the DL and UL, respectively.

The left plot, in Figure 12a shows normalized downlink (DL) bit rate for the 4x4 antenna configuration as a function of the separation given in wavelengths, λ , between the two BS antenna columns. Three different metrics are shown; cell throughput, cell edge bit rate and peak bit-rate. These metrics are defined by the average cell throughput and the 5- and 95-percentile of the CDF of the active radio link bit rate (ARLBR), respectively. The ARLBR is the user bit rate averaged over the time a user has been assigned resources. The bit rates have been normalized in such a way that it is one at 1λ separation between the dual-polarized BS antennas for each curve. The results in the left plot (a) show that the cell throughput and cell edge bit rate decrease as the base station’s antenna separation increases, while it is essentially constant for peak rate. There is a benefit of a small antenna separation in this scenario since it is interference limited; hence, beamforming gains are more important than spatial multiplexing gains. The middle plot, (b), shows results from the 4x4 antenna configuration of the probability of a certain transmission rank as a function of the two dual-polarized antennas separation. The rank statistics in the middle plot show that rank 1 and 2 are most probable for small antenna separation. As the separation increases, the probability of rank 3 transmission increases. Almost no rank 4 transmissions occur, since the signal-to-interference-and-noise ratio (SINR) is too low in this scenario.

Corresponding UL results for a 1x4 configuration are shown in Figure 12c. The results show that in this case the bit rate increases (except for the cell edge bit rate at 10λ as the separation between the dual-

polarized antennas increases. This is because the diversity gain increases with increased co-polarized antenna separation.

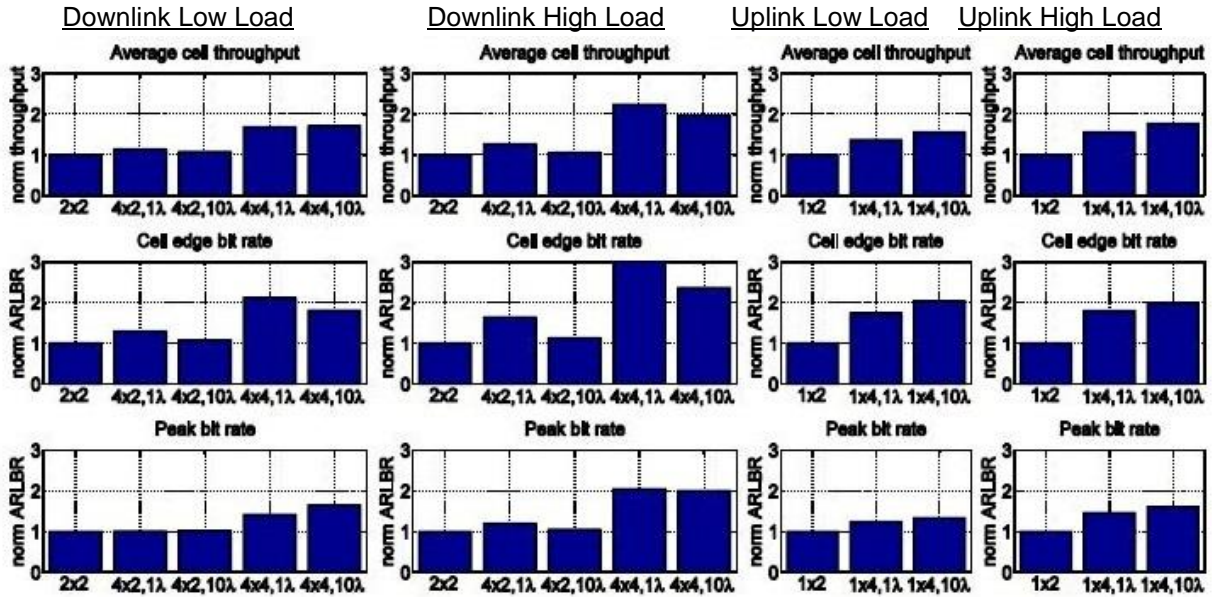


Figure 13 – Performance summary of different antenna configurations for DL and UL for networks in high or low load conditions.

Figure 13 shows a summary of the performance with different configurations for DL and UL in networks with high load, as well as in networks with low load. The bit rates have been normalized to the 2x2 and 1x2 results for DL and UL, respectively. Two different antenna separations are compared: 1λ and 10λ, representing small and large separation, respectively. In the low load network scenarios shown, there are on average 0.1 UEs/cell. The results show that for DL, a small antenna separation gives highest performance for all cases except for peak throughput at low load. For UL, large antenna separation gives highest performance in all cases. However, most of the UL gain in going from two to four antennas is achieved also with 1λ separation.

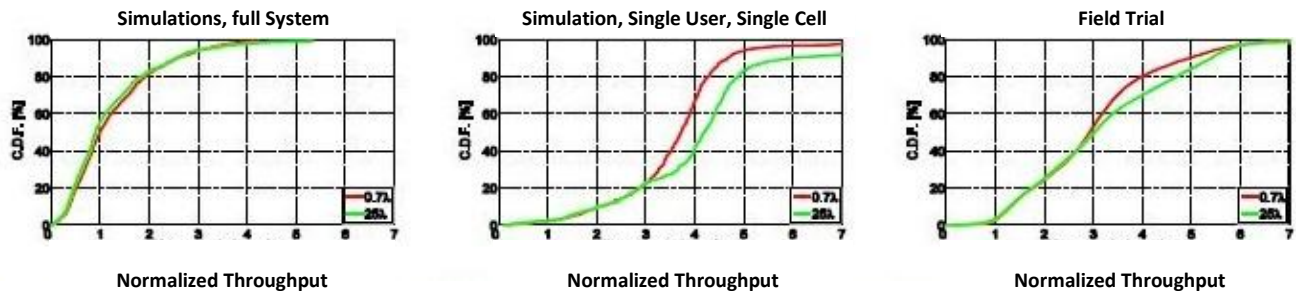


Figure 14 – Results from full system simulation (left), single cell, single user simulation (middle) and field trial (right) for downlink 4x4 antenna configuration. Green curves correspond to 25 wavelength spacing; red curves correspond to 0.7 wavelengths.

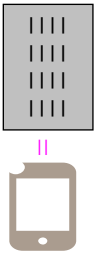
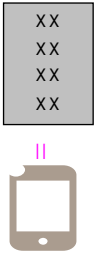
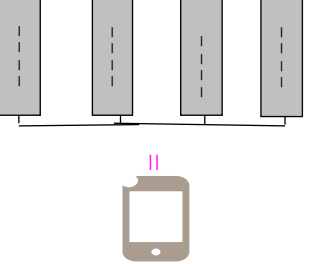
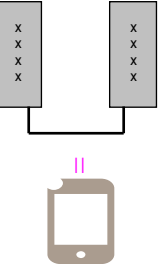
In order to allow comparison to measurement results, Figure 14 shows throughput CDFs for a full system simulation with an average of 4 UEs/cell, simulation of a single UE single cell (SUSC) scenario, and for the SUSC field trial results, respectively. These results are for 4x4 configurations and each plot shows CDFs for two antenna separations; 0.7 and 25. The results are normalized to the median of the full system simulation CDF for the antenna separation of 0.7. The measurements were performed using a single UE in a single cell scenario and only downlink performance was addressed.^{xi} In order to simulate a SUSC scenario, all intercell interference was turned off in the simulator. In these simulations, somewhat different parameter settings were used to better reflect the trial scenario, e.g., getting a similar signal-to-noise ratio (SNR) range in simulations and trials. The purpose of the comparison is not to reach an accurate agreement in terms of absolute performance numbers, but rather to illustrate that the relative performance between different configurations shows similar behavior.

2.5 ANTENNA ARRAY CALIBRATION

The effect of calibration on some of these various antennas schemes was also considered with the following results obtained for some selected schemes. Here we see that closely spaced antennas suffer slightly more than widely spaced antennas from lack of calibration. The effects are in the range of a 6% to 2% reduction in spectral efficiency for the un-calibrated scenario in the simulation model used in this study.⁵

⁵ The simulation parameters were the same as described in the previous footnote for the performance comparison of the various antenna schemes, but with the un-calibrated base station antennas corresponding to uniformly random phase offsets applied to the transmit signals at the antenna ports. This has the effect of equalizing the PMI uplink reports.

Impact of 'Uncalibrated BS antenna' Assumption

	ULA-4V	CLA-2X	DIV-4V	DIV-2X
Configuration				
SE CBTP Perf. Calibrated	2.4 790	2.2 740	2.1 660	2.1 680
absolute impact [%] Uncalibrated	-6% -11%	-4% -3%	-3% -2%	-2% -3%
SE CBTP Gain [%] Calibrated	28% 38%	20% 30%	15% 18%	13% 20%
Uncalibrated	19% 23%	15% 27%	12% 15%	11% 15%
Impacted by Uncalibration	Higher	Moderate	Lower	Lower

Martin Schipporeit, Feb. 2013

Figure 15 – Impact on Spectral Efficiency (SE) and Cell Border Through Put (CBTP) due to lack of calibration of the base station's antenna paths. As before, these simulation results are an average of several configurations of environmental parameters and specific instances vary considerably, so field experience may vary similarly from one instance to another. These simulations provide insights into comparative performance more than absolute expectations.

Similar to previous results, the full system simulation shows that a small antenna separation gives the highest throughput. In the Single User-Single Cell (SUSC) simulation and the field trial, the configuration with large antenna separation gives higher throughput for UE positions with good channel quality. In these cases, the SNR is sufficiently high to benefit from the additional spatial multiplexing gains offered by the uncorrelated antennas.

Antenna arrays that are used to perform the various forms of beamforming or antenna precoding described in this white paper generally require some form of calibration to control the relative amplitude and phase values on the transceivers that drive the antenna array. (Note that we are distinguishing antenna precoding from beamforming by using the term precoding to refer specifically to the TM modes in LTE, for example that perform UE-specific beamforming at baseband based on PMI-fed back (as in TM4 or TM9) or Sounding Reference Signals (SRS) (as in TM7 or TM8). In general, errors in amplitude and/or phase response in the transceivers behind the array can degrade the performance of the beamforming or precoding, and the level of degradation depends on the particulars of the beamforming or precoding strategy and the associated calibration strategy being used.

This section describes the antenna array calibration requirements for three common situations. The first subsection describes the calibration requirements for a beamforming antenna array where the important issues of concern are the key characteristics of the antenna array radiation pattern, most notably the beamforming gain and sidelobe behavior of the overall array. The second and third subsections describe the calibration requirements for antenna arrays involved in adaptive per-user precoding where the precoding weights are applied at baseband and the key metrics of concern are the quality of the overall link between the transmit array at the base station and the UE (e.g., TM4, TM7, TM8, or TM9 in LTE). The second section deals with how calibration errors can actually degrade the performance of codebook-feedback based precoding for Single-User MIMO (e.g., TM4, TM9) as well as for Multi-User MIMO (e.g., TM9). The third section deals with how calibration errors in TDD can degrade the performance of SRS-based precoding (e.g., TM7, TM8 in LTE) that leverages the UL/DL reciprocity of a TDD system.

2.5.1 CALIBRATION REQUIREMENTS FOR BEAMFORMING

Beamforming quality depends on the relative accuracy of the amplitude and phase values of each transceiver. As with all multi-column beamforming antenna systems, there is some degree of error due to undesirable variations between each transmit and receive path. With beamforming, some type of calibration method must be implemented to minimize the amplitude and phase errors between transceivers and antenna columns. Figure 16, below, shows the comparison of a beam synthesized without any amplitude or phase errors as compared to a beam synthesized with random amplitude and phase errors. For this particular example, random amplitude errors of $\pm 0.5\text{dB}$ and random phase errors of $\pm 20^\circ$ were applied simultaneous to each transceiver of an 8-column beamforming antenna array.

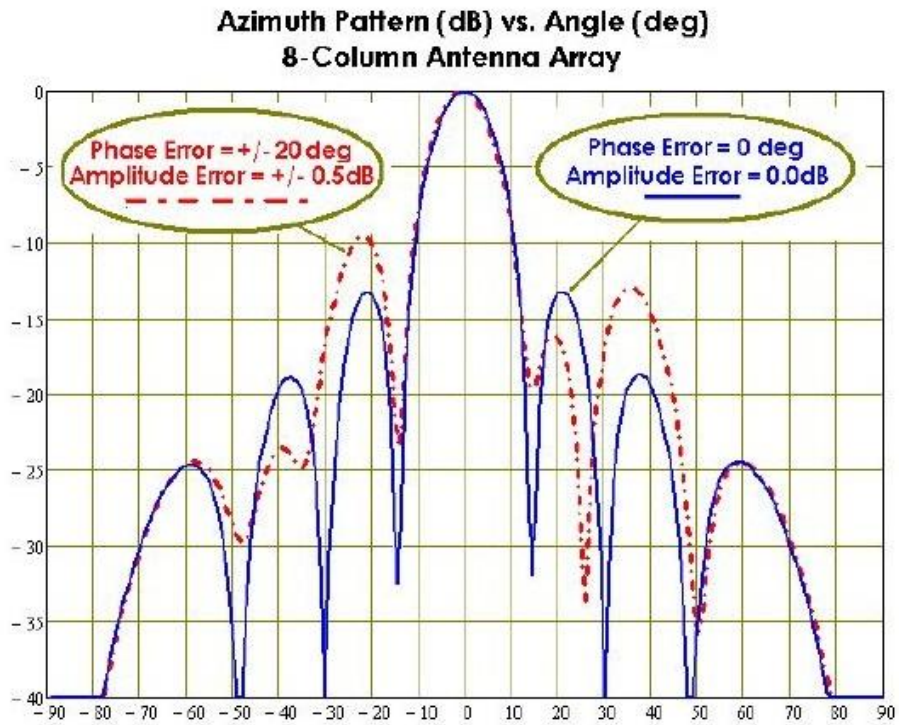


Figure 16 – Beamforming degradation due to amplitude and phase errors.

As can be seen in the patterns in Figure 16, phase and amplitude errors can result in significant beamforming degradation. The degraded patterns may result in undesirably high side-lobe levels, squinting of the main beam, and degradation in gain, as well as losing the ability to accurately position nulls. Typical beamforming systems deployed today require that amplitude variations be limited to +/- 0.5dB, while phase variations are limited to no more than +/- 5 degrees.

Calibration networks for beamforming antennas can be implemented by integrating directional couplers on individual antenna paths. The coupled outputs are then combined and connect to a dedicated calibration transceiver. A typical calibration network block diagram for a 4-column beamforming antenna array is shown below in Figure 17. By selectively powering up individual transceivers, the amplitude and phase characterization of each antenna path can be achieved.

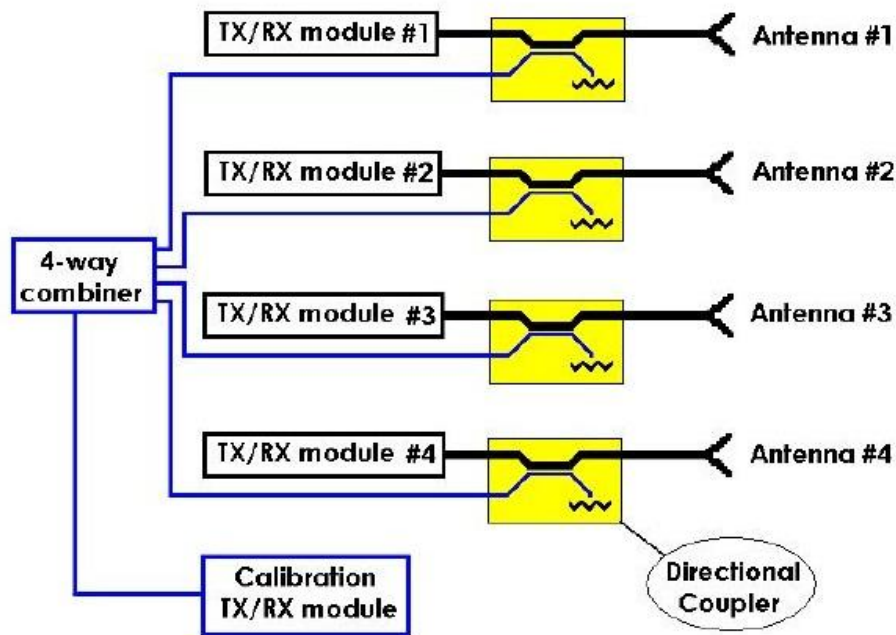


Figure 17 – Calibration network block diagram for a 4-column beamforming array.

The calibration network shown in Figure 17 allows for periodic automated calibrations. Typically, these calibrations would take place at periods of low traffic usage, but essentially can be performed at any time. It is important to note that the power divider network and directional couplers must be carefully designed and calibrated such that they do not contribute additional amplitude and phase errors. These types of networks require careful s-parameter characterization at the factory level to ensure that adequate performance levels are achieved.

For beamforming antennas with additional columns, there will be an obvious increase in cost and complexity of the calibration networks. Some lower cost calibration networks have eliminated the need for couplers, combiners and dedicated calibration transceivers. These lower cost calibration networks exploit the strong mutual coupling of the adjacent antenna columns to establish phase relationships between columns. A separate calibration transceiver is not required in TDD systems, but instead, the main transceivers are used for calibration activity. While these types of calibration networks are lower cost and lower complexity, they do require more complex algorithms for extracting the calibration data.

It is important to note that the amplitude and phase errors are proportional to the operating frequency. Beamforming antenna systems operating at 2.5 GHz and 3.5 GHz will observe phase variation significantly higher than for a system operating at 850MHz. These increased errors are due to the natural tolerance variations of the transmission line paths at higher frequencies.

2.5.2 EFFECT OF CALIBRATION ERRORS IN DL SU-MIMO AND DL-MU-MIMO WITH CODEBOOK-FEEDBACK-BASED PRECODING

As mentioned in Section 2, LTE Releases 8 through 10 support two main forms of closed-loop MIMO on the downlink: Single User MIMO (SU-MIMO) and multi-user MIMO (MU-MIMO). The term “closed-loop” refers to how the DL MIMO methods employ some level of knowledge of the downlink channel to perform beamforming of one or more data streams to either one user at a time (SU-MIMO) or to two or more users at a time (MU-MIMO). Typically, Precoder Matrix Indication (PMI) is computed by the UE and feedback to the eNB, and the eNB can either apply the transmit beamforming weights indicated by the PMI directly (e.g., in the case of SU-MIMO) or the eNB can compute vendor-specific transmit beamforming weights based on the PMI feedback (e.g., in the case of MU-MIMO). In PMI feedback, a codebook of possible transmit beamforming matrices is maintained at both the eNB and the UE, and the UE selects and feeds back the PMI that corresponds to the preferred transmit beamforming matrix that will optimize the downlink performance for the UE.

During downlink data transmission, the beamforming or precoding weights for DL-SU-MIMO and DL-MU-MIMO are generally applied in the frequency domain at baseband prior to up-mixing to RF. As a result, for optimal performance the precoding weights must be optimized for a channel that includes the baseband-to-RF conversion process at the transmit array in addition to the RF multipath channel between the physical antennas and the UE(s). When DL-SU-MIMO and MU-MIMO is performed based on PMI feedback, the UE computes the preferred PMI based on an estimate of the downlink channel that includes the baseband-to-RF up-mixing and the RF multipath channel. As a result, the PMI is optimized for the actual channel over which the DL data will be transmitted. However, the codebooks in LTE were designed assuming the transmit array was a “calibrated” array, where the term “calibrated” is used here to mean a transmit array in which the transmit hardware responses do not modify the spatial nature of the overall channel response between the baseband at the transmit array and the receive antennas. In a calibrated array, the transmit branches all effectively have identical frequency responses (to within a common complex constant) from baseband to the physical antenna ports at RF. In an un-calibrated array, the frequency responses on the transmit branches may be different, which will cause the statistical characteristics of the overall downlink channel to deviate from those seen with a calibrated array. As a result, with an un-calibrated transmit array, the performance of the codebook feedback-based DL transmissions will be affected since the codebooks in Rel-8 and Rel-10 were designed to span the RF multipath channels seen by calibrated arrays.

In a realistic implementation of a transmit array at an eNB, there are a variety of factors that will cause a transmit array to be un-calibrated. Two of these factors studied in 3GPP^{xvi} and ^{xvii} are wideband phase errors and time alignment errors. Time alignment errors (TAE) are timing differences between the transmit branches and cause the signal transmitted on each branch to be transmitted with a different delay. The different time delays cause each transmit branch to have a different frequency-selective phase ramp across the transmitted signal bandwidth, where the rate of change of the phase across the bandwidth is proportional to the relative time delay of the branch. As a result, these different phase ramps cause the overall spatial channel response between the baseband of the transmit array and the UE to vary more rapidly across the frequency bandwidth than it otherwise would. In DL SU- and MU-MIMO, a single set of precoding transmit weights are typically applied across a data allocation and are therefore unable to track any channel response variations that occur within the allocation. Therefore, any increase in the channel response variations across the allocation will degrade the performance of SU- and MU-MIMO in wideband allocations due to the inability to track those variations. Narrowband allocations tend to suffer less degradation than wideband allocations due to less channel response variation across a smaller allocation. MU-MIMO transmission tends to suffer more degradation than SU-

MIMO due to the need to accurately point nulls to minimize the cross-talk received at multiple UEs. Even though the degradations with time alignment errors are more severe in wideband allocations than in narrowband allocations, narrowband precoding in narrowband data allocations does not appear to fully mitigate the time alignment problem in all cases (see [xviii]).

Another factor studied in 3GPP is wideband phase errors on the transmit branches. Even if all the branches of the transmit array are perfectly time aligned, each transmit branch may still have a different gain and phase response due to a variety of implementation-specific factors. In 3GPP, a simplistic model for wideband phase errors was used where the frequency response on each transmit branch was modeled to be constant in amplitude across frequency with a random phase that is fixed in time and non-selective frequency. Unfortunately, a realistic implementation may have variations in the overall frequency response of the different transmit branches that are more complicated to model than a simple random wideband phase error term across the branches.

In 3GPP, a simulation study was performed to assess the magnitude of the degradations that occur when time misalignment and wideband phase errors cause the transmit branches to be un-calibrated. The presence of these calibration errors result in overall channel responses that the LTE codebooks may not span well (this effect is called the codebook quantization error problem), which was shown to be a bigger problem for MU-MIMO than SU-MIMO given the accuracy required in MU-MIMO to point nulls for effective cross-talk mitigation. It was shown in [xix] that the performance of SU-MIMO was relatively insensitive to time alignment and wideband phase errors. However, DL-MU-MIMO performance was often severely degraded by such errors. Wideband phase errors generally cause only minor degradations in MU-MIMO transmission with the exception of uniform linear arrays operating in line-of-sight channels, in which case the degradations are severe. With narrowband allocations, time misalignment errors tend to cause only minor degradations with the exception of a uniform linear array operating in line of sight channels, where the degradations are severe. With wideband allocations, time misalignment often causes extreme levels of performance loss from the performance with perfectly calibrated transmit arrays.

2.5.3 CALIBRATION REQUIREMENTS FOR RECIPROcity-BASED PRECODING IN TDD SYSTEMS

In static Time-Division Duplex (TDD) channels, the propagation environment is known to be reciprocal in uplink and downlink due to both uplink and downlink occupying the same bandwidth on the same carrier frequency. In TDD systems (e.g., LTE TM7 and TM8), a common technique for transmit precoding is to measure the uplink channel responses to a particular subscriber (e.g., by leveraging the Sounding Reference Signals transmitted by the UE) and use the measured uplink channel responses as an estimate for the downlink channel. The transmit weights used by the transmit beam former are then calculated based on the estimated downlink channel response. Although the uplink and downlink RF channel responses are reciprocal (assuming no time variations in the channel between uplink and downlink), the transmit and receive hardware at the base station are generally not reciprocal. The uplink channel measured by the base station includes the base station receive hardware and the subscriber transmit hardware; while the downlink channel through which the beamforming is performed includes the base station transmit hardware and the subscriber receive hardware. Unless a calibration is performed, the transmit and receive hardware across an antenna array are generally not identical in their gain and phase responses, and the differences must be accounted for by any transmit array algorithm that leverages UL/DL reciprocity. This accounting for the transmit and receive hardware is the essence of the calibration problem for reciprocity-based antenna arrays. Typically, a base station that exploits uplink/downlink reciprocity in TDD will have a calibration mechanism for insuring that the spatial channel measured on the baseband of the uplink is equivalent to the downlink spatial channel over which the

transmit beamforming will be performed. References [xx], [xxi], and [xxii] provide an overview of the reciprocity calibration problem and propose a methodology for reciprocity calibration. Other techniques for reciprocity calibration are possible, and generally the calibration mechanism is a vendor-specific function. Typically a reciprocity calibration mechanism will involve first measuring the forward and reverse path gains of the transceiver hardware and then compensating for the forward and reverse differences when computing the downlink transmit beamforming weights. The calibration mechanism is typically not something that has to be performed very often because the variations in the hardware responses are generally caused by changes in temperature and other slowly varying factors.

It is important to also point out that while the TDD channel is substantially reciprocal, the intercell interference in the system is not, and the beamforming from using a conjugate mirror approach does not consider interference levels or the utility of null forming in the direction of interferers. Consequently, the conventional wisdom that TDD has more MIMO potential than FDD is diluted considerably.

SUMMARY

This paper has provided practical details, based upon the latest LTE information on the significant gains in the efficient use of MIMO and general antenna schemes, many of which have also been utilized for HSPA systems. The paper detailed the MIMO techniques and antenna configurations that have helped meet the huge growth in mobile broadband demand. The relative advantages of closely spaced Clustered Linear Arrays were shown compared with diversity schemes with more widely spaced antenna radomes, and the close performance seen with arrays of vertical antennas versus cross polarized antennas was examined and explained. Calibration tradeoffs and complexities were also described.

These lessons, both from simulations and from field measurements, are guiding the deployment of CLA-2X, CLA-4X as well as DIV-8V systems worldwide, where tradeoffs between antenna radome size and performance are considered.

We continue to see the growing importance of not only smart antennas, but the smart application of antenna technologies of all sorts, and we are reminded of the impressive strides in the understanding and state of the art of antenna technologies and the signal processing associated with them. No doubt, the coming years will see further advances in their use.

DEFINITIONS AND ACRONYMS

Term	Definition	Units
1st Upper Sidelobe Level	Level of the 1st sidelobe on the upper half space of the elevation pattern relative to the main beam peak level.	dB
3rd Order PIM (Passive Intermodulation)	3rd order intermod products using two 20W (2 x 43dBm) carriers; 3rd order product defined at frequencies of (F1 +/- 2*F2) and (F2 +/- 2*F1) falling within the receive band when transmit frequencies F1 and F2 are used as the input carriers. The output is typically specified to be -150dBc or better.	dBc
Integrated Antenna/Radio	Active Antenna – with power amplifier, LNA, filter and CPRI connection integrated into one radome. This is a special case of the more capable AAS antenna array insofar as it only controls the horizontal directions of the beams/MIMO parameters.	
AAS	Active Antenna System – a two dimensionally controlled array of antenna elements, each with their own radio, power amplifier, filters and LNA so that beams or complex weights can be applied to the antenna array in both horizontal as well as vertical directions, suitable for “3D-beamforming.” This is a two dimensional extension of the simpler Integrated Antenna/Radio concept.	
AISG	Antenna Interface Standards Group Specified interface control signals for RET and RAZ as well as power.	
Azimuth Beam peak	Beam pointing angle (in Azimuth plane) defined using center of 3dB points; referenced to a mechanical boresight.	degrees
Azimuth Beamwidth	Typically stated as 3dB beamwidth (unless otherwise specified); Defined as the angular width of the azimuth (horizontal) pattern, including beam maximum, between points 3dB down from beam max level.	degrees
Azimuth Fan Range	Range of Azimuth Beamwidths achievable by the antenna device.	degrees
Azimuth Pan Range	Angular range of azimuth beampeaks through which the azimuth pattern will sweep MECHANICALLY via physical movement of the antenna device (usually defined as +/- X from boresight direction).	degrees
Azimuth Roll-off	Pattern level defined at the sector edge angles relative to mechanical boresight (adjusted for azimuth pan angle offset) where the sector is defined as follows: * For a nominal Azimuth Beamwidth of 45deg or Narrower (i.e. 33/45), a 60deg sector is defined (-30/+30deg sector). * For a nominal Azimuth Beamwidth Wider than 45deg (i.e. 65/85), a 120deg sector is defined (-60/+60deg sector).	dB
Azimuth Scan Range	Angular range of azimuth beampeaks through which the azimuth pattern will sweep ELECTRICALLY with the antenna device fixed (usually defined as +/- X from boresight direction, azimuth counterpart to elevation beamtilt range).	degrees
Band-to-Band Squint	Measured as max angular deviation between overlay of AZ patterns for 2 ports in different frequency bands of a single or dual pol antenna - mechanical boresight required for a single port in a single band, all other ports/bands measured from same mechanical boresight.	degrees

Band-to-Band Tracking	Measured at max magnitude deviation over the defined sector (adjusted for azimuth pan angle offset) of AZ pattern overlay for 2 ports in different frequency bands of a single or dual pol antenna - mechanical boresight required for a single port in a single band, all other ports/bands measured from same mechanical boresight The sector is defined as follows: * For a nominal Azimuth Beamwidth of 45deg or Narrower (i.e. 33/45), a 60deg sector is defined (-30/+30deg sector). * For a nominal Azimuth Beamwidth Wider than 45deg (i.e. 65/85), a 120deg sector is defined (-60/+60deg sector).	dB
Beam Tilt	Defined using center of 3dB points; referenced to a mechanical boresight.	degrees
Beam Tilt Range	Defined as the range of angles - min-to-max - that the antenna will scan in the EL pattern.	degrees
CLA Clustered Linear Array Antennas	Family of clustered linear antenna configurations such as those resulting from forming clusters of closely spaced antenna elements while separating these clusters either by widely spacing them or by different polarizations.	
Connector Location	Physical mounted location of antenna port connectors: Bottom, Back.	N/A
Connector Type	Type of Connector used on antenna port (s) Typically DIN 7/16.	N/A
CPRI	Common Public Radio Interface™ Specification of interface from base band unit to remote radio heads.	
DIV array antennas	Family of diversity antenna configurations such as those resulting from all elements being widely spaced or separated by different polarizations.	
Elevation Beamwidth	Typically stated as 3dB beamwidth (unless otherwise specified); Defined as the angular width of the elevation (vertical) pattern, including beam maximum, between points 3dB down from beam max level.	degrees
Frequency Range	Operating frequency band the antenna will perform to spec over.	MHz
Front-to-Back Ratio (co-pol only)	Pattern level discrimination measured at 180deg relative to azimuth beam pointing angle – > determined using Co-pol Azimuth pattern only.	dB
Front-to-Back Ratio, Angular Region (total power)	Pattern level discrimination measured over an angular back region defined as 180deg +/- 30deg relative to azimuth beam pointing angle – > determined using Total Power Azimuth patterns (achieved via vector sum addition of co-pol & x-pol patterns).	dB
Front-to-Back Ratio, Angular Region (co-polarized only)	Pattern level discrimination measured over an angular back region defined as 180deg +/- 30deg relative to azimuth beam pointing angle – > determined using Co-pol Azimuth patterns only.	dB
Front-to-Side Ratio	Pattern level discrimination defined at +/-90deg relative to mechanical boresight (adjusted for azimuth pan angle offset) in the Azimuth co-pol pattern.	dB
Gain	Measured antenna gain using a Swept Frequency Gain-by-Comparison method (std procedure) involving a Standard Gain Antenna with Published Absolute Gain.	dBi

H/V Tracking	Discrimination between H-pol & V-pol AZ pattern over the defined sector (adjusted for azimuth pan angle offset) of AZ pattern component cuts for x-pol antennas where the sector is defined as follows: * For a nominal Azimuth Beamwidth of 45° or narrower (i.e. 33/45), a 60° sector is defined (-30/+30° sector). * For a nominal Azimuth Beamwidth Wider than 45° (i.e. 65/85), a 120° sector is defined (-60/+60° sector).	dB
Impedance	50 ohm system reference	ohms
Maximum Upper Sidelobe Level	Level of the maximum sidelobe on the upper half space of the elevation pattern from horizon to zenith relative to the main beam peak level.	dB
MBSFN	Multicast Broadcast Single Frequency Network. When common Enhanced Multi-Media Broadcast Multicast Service(eMBMS) is transmitted by multiple base stations all on a single frequency carrier, the network is said to us MBSFN.	
Null Fill	Defined as the depth of the 1st null in the lower half space of the elevation pattern relative to the main beam peak level - typically defined as the 1st lower null fill between the main lobe and 1st lower sidelobe.	dB
ORI	Open Radio Equipment Interface, an ETSI standards effort is a direct result of requirements work undertaken by the NGMN Alliance, in their OBRI (Open BBU RRH Interface) project. It extends the CPRI work to include Synchronization, L1, HDLC, Ethernet and vendor specific signaling.	
Polarization	Definition of antenna port(s) polarization: +/- 45° Slant, Hor, Vert, Hor/Vert, LHCP, RHCP.	degrees
Port-to-Port Isolation (In-band / Intra-band / Intra-system)	Isolation between 2 antenna ports within the same frequency band.	dB
Port-to-Port Isolation (X-band / Inter-band / Inter-system)	Isolation between 2 antenna ports in a multiple band system across separate frequency bands (co-pol & x-pol port configurations).	dB
Port-to-Port Squint	Measured as max angular deviation between overlay of AZ patterns for 2 ports of a x-pol antenna - mechanical boresight required for a single port, all other ports measured from same mechanical boresight.	degrees
Port-to-Port Tracking	Measured at max magnitude deviation over the defined sector (adjusted for azimuth pan angle offset) of AZ pattern overlay for 2 ports of a x-pol antenna - mechanical boresight required for a single port, all other ports measured from same mechanical boresight where the sector is defined as follows: * For a nominal Azimuth Beamwidth of 45deg or Narrower (i.e. 33/45), a 60deg sector is defined (-30/+30deg sector). * For a nominal Azimuth Beamwidth Wider than 45deg (i.e. 65/85), a 120deg sector is defined (-60/+60deg sector).	dB
Power Handling (per port)	Max CW Power Level per single port input specified at an ambient room temperature of 20°C enduring a continuous 1 hour power soak.	Watts
Power Handling (total power)	Max CW Power Level split equally into two ports of a dual-pol antenna (same antenna system) specified at an ambient room temperature of 20°C enduring a continuous 1 hour power soak.	Watts

Power Handling at Elevated Temp (per port)	Max CW Power Level per single port input specified at an ambient temperature of 46° Celsius enduring a continuous 1 hour power soak.	Watts
Power Handling at Elevated Temp (total power)	Max CW Power Level split equally into two ports of a dual-pol antenna (same antenna system) specified at an ambient temperature of 46° Celsius enduring a continuous 1 hour power soak.	Watts
Power Handling at Max Operating Temp (total power)	Max CW Power Level split equally into two ports of a dual-pol antenna (same antenna system) specified at a maximum operating temperature of 65° Celsius enduring a continuous 1 hour power soak.	Watts
RAZ	Remote AZimuth control.	°
RET	Remote Electrical Tilt.	° downtilt (positive down)
Return Loss	Listed Spec; Production Spec = Listed Spec + 0.5dB margin safety factor.	dB
Tilt Accuracy	Defined as the accuracy of a given beam tilt angle per the specified downtilt of the antenna - for variable tilt, referenced to the tilt indicator defined by the label.	degrees
ULA Uniform Linear Array Antennas	Family of uniform linear array antenna configurations such as those resulting from all elements being uniformly closely spaced. E.g. ULA-2V has two columns of vertically polarized antenna elements.	
Upper Sidelobe Suppression (USLS)	Level of the highest sidelobe within the first 20deg of the upper half space of the elevation pattern above horizon relative to the main beam peak level.	dB
X-pol Level	Relative level of x-pol referenced to co-pol beam maximum defined at a given angle.	dB
X-pol Level (over Sector)	Maximum level of x-pol referenced to co-pol beam maximum over the defined sector (adjusted for azimuth pan angle offset) for a given port where the sector is defined as follows: * For a nominal Azimuth Beamwidth of 45deg or Narrower (i.e. 33/45), a 60deg sector is defined (-30/+30deg sector). * For a nominal Azimuth Beamwidth Wider than 45deg (i.e. 65/85), a 120deg sector is defined (-60/+60deg sector).	dB
X-pol Ratio (Discrimination) on Boresight	Discrimination between co-pol & x-pol AZ pattern levels at mechanical boresight (adjusted for azimuth pan angle offset) for a given port.	dB
X-pol Ratio (Discrimination) over Sector	Discrimination between co-pol & x-pol AZ pattern levels at all angles over the defined sector (adjusted for azimuth pan angle offset) for a given port where the sector is defined as follows: * For a nominal Azimuth Beamwidth of 45deg or Narrower (i.e. 33/45), a 60deg sector is defined (-30/+30deg sector). * For a nominal Azimuth Beamwidth Wider than 45deg (i.e. 65/85), a 120deg sector is defined (-60/+60deg sector).	dB

REFERENCES

- ⁱ What base station antenna configuration is best for LTE-Advanced?, By Julius Robson, Kevin Linehan, COMMSCOPE White Paper WP-106096-EN (9/12). (Note that this paper predated Rel. 8 and 9 of the 3GPP standard.) Available on-line April 2013 at:
http://docs.commscope.com/Public/What_BSA_configuration_is_best_for_LTE-Advanced.pdf
- ⁱⁱ Schmidt, R.; , "Multiple emitter location and signal parameter estimation," *Antennas and Propagation, IEEE Transactions on* , vol.34, no.3, pp. 276- 280, Mar 1986 doi: 10.1109/TAP.1986.1143830
URL: <http://ieeexplore.ieee.org/stamp/stamp.jsp?tp=&arnumber=1143830&isnumber=25667>.
- ⁱⁱⁱ Roy, R; Paulraj, A; Kailath, T; "ESPRIT--A subspace rotation approach to estimation of parameters of cisoids in noise,"*IEEE Transactions on Acoustics Speech and Signal Processing*, Oc. 1986, Vol 34, issue 5, page 1340-1342.
- ^{iv} A.M.D. Turkmani, A.A. Arowajolu, P.A. Jefford, and C.J. Kellett, "An Experimental Evaluation of the Performance of Two-Branch Space and Polarization Diversity Schemes at 1800 MHz," *IEEE* 0018-9545/94404,00, 1995.
- ^v Brian S. Collins, "The Effect of Imperfect Antenna Cross-Polar Performance on the Diversity Gain of a Polarization-Diversity Receiving System," *Microwave Journal*, April 2000.
- ^{vi} R. Bhagavatula, R. W. Heath, Jr., and K. Linehan, "Performance Evaluation of MIMO Base Station Antenna Designs," *Antenna Systems and Technology Magazine*, vol. 11, no. 6, pp. 14 -17, Nov/Dec. 2008.
- ^{vii} Product data sheet available at: <http://www.argusantennas.com/products/data-sheets/Multi-Beam-Antennas/2x9NPA2010F.pdf>
- ^{viii} Bhagavatula, Ramya, Robert W. Heath Jr, and Kevin Linehan. "Performance evaluation of MIMO base station antenna designs." *Antenna Systems and Technology Magazine* 11, no. 6 (2008): 14-17. URI: http://docs.commscope.com/Public/performance_evaluation_MIMO_base_station_antenna_designs.pdf
- ^{ix} Martin Schipporeit, internal communications, Alcatel-Lucent. February 2013
- ^x F. Athley, M. Alm, O. Kaspersson, K. Werner, J. Furuskog, and B. Hagerman, "Dual-Polarized Base Station Antenna Configurations for LTE," to appear in Proc. 2010 IEEE International Symposium on Antennas and Propagation.
- ^{xi} K. Werner, J. Furuskog, M. Riback, and B. Hagerman, "Antenna Configurations for 4x4 MIMO in LTE—Field Measurements," to appear in Proc. IEEE VTC Spring 2010.
- ^{xii} "Spatial Channel Model for Multiple Input Multiple Output (MIMO) Simulations," 3GPP TR 25.996, V7.0.0, available on line at <http://www.3gpp.org/FTP/Specs/html-info/25996.htm>.
- ^{xiii} L. Wan, S. Tsai, and M. Almgren, "A Fading-Insensitive Performance Metric for a Unified Link Quality Model," Proc. IEEE WCNC, 2006. Available on-line at:
<http://ieeexplore.ieee.org/stamp/stamp.jsp?arnumber=01696622>.
- ^{xiv} "Physical Layer Aspects for Evolved Universal Terrestrial Radio Access (UTRA)," 3GPP TR 25.814, V7.1.0, section A.2, available on line at <http://www.3gpp.org/FTP/Specs/html-info/25814.htm>.

-
- ^{xv} Section 7.1 of 3GPP Section 7.1 of TS 36.101 V8.7 states: "The requirements in Section 7 assume that the receiver is equipped with two Rx port as a baseline. Requirements for 4 ports are FFS. With the exception of clause 7.9 all requirements shall be verified by using both (all) antenna ports simultaneously." Available on line at: <http://www.3gpp.org/ftp/Specs/html-info/36101.htm> last accessed on April 18, 2010.
- ^{xvi} R1-113153 – "Discussion of Time Misalignment and Antenna Array Calibration," Nokia Siemens Networks, Nokia, 3GPP TSG-RAN WG1#66bis, Zhuhai, China, Oct 10-14, 2011. Available on-line at: http://www.3gpp.org/ftp/tsg_ran/WG1_RL1/TSGR1_66b/Docs/R1-113153.zip
- ^{xvii} R1-114328 – "Performance Characteristics of SU-MIMO and MU-MIMO with Time Misalignment and Wideband Phase Calibration Errors," Nokia Siemens Networks, Nokia, 3GPP TSG-RAN WG1#67, San Francisco, CA, USA, Nov14-18, 2011. Available on-line at: http://ftp.3gpp.org/ftp/tsg_ran/WG1_RL1/TSGR1_67/Docs/R1-114328.zip
- ^{xviii} R1-113153, Oct 10-14, 2011, "Discussion of Time Misalignment and Antenna Array Calibration," Last accessed June 25, 2012. URI: http://www.3gpp.org/ftp/tsg_ran/WG1_RL1/TSGR1_66b/Docs/R1-113153.zip
- ^{xix} R1-114328, Nov 14-18, 2011. "Performance Characteristics of SU-MIMO and MU-MIMO with Time Misalignment and Wideband Phase Calibration Errors." Last Accessed June 25, 2012. URI: http://www.3gpp.org/ftp/tsg_ran/WG1_RL1/TSGR1_67/Docs/R1-114328.zip
- ^{xx} Bourdoux, A.; Come, B.; Khaled, N.; , "Non-reciprocal transceivers in OFDM/SDMA systems: impact and mitigation," Radio and Wireless Conference, 2003. RAWCON '03. Proceedings , vol., no., pp. 183-186, 10-13 Aug. 2003 doi: 10.1109/RAWCON.2003.1227923 URL: <http://ieeexplore.ieee.org/stamp/stamp.jsp?tp=&arnumber=1227923&isnumber=27540>
- ^{xxi} Liu, J.; Bourdoux, A.; Craninckx, J.; Wambacq, P.; Come, B.; Donnay, S.; Barel, A.; , "OFDM-MIMO WLAN AP front-end gain and phase mismatch calibration," Radio and Wireless Conference, 2004 IEEE, vol., no., pp. 151- 154, 19-22 Sept. 2004 doi: 10.1109/RAWCON.2004.1389095 URL: <http://ieeexplore.ieee.org/stamp/stamp.jsp?tp=&arnumber=1389095&isnumber=30232>
- ^{xxii} Liu, J.; Bourdoux, A.; Craninckx, J.; Come, B.; Wambacq, P.; Donnay, S.; Barel, A.; , "Impact of front-end effects on the performance of downlink OFDM-MIMO transmission," Radio and Wireless Conference, 2004 IEEE , vol., no., pp. 159- 162, 19-22 Sept. 2004 doi: 10.1109/RAWCON.2004.1389097 URL: <http://ieeexplore.ieee.org/stamp/stamp.jsp?tp=&arnumber=1389097&isnumber=30232>

ACKNOWLEDGEMENTS

The mission of 4G Americas is to promote, facilitate and advocate for the deployment and adoption of the 3GPP family of technologies throughout the Americas. 4G Americas' Board of Governor members include Alcatel-Lucent, América Móvil, AT&T, Blackberry, Cable & Wireless, Cisco, CommScope, Entel, Ericsson, Gemalto, HP, Mavenir Systems, Nokia Siemens Networks, Openwave Mobility, Powerwave, Qualcomm, Rogers, T-Mobile USA and Telefónica.

4G Americas would like to recognize the project leadership and important contributions of Stephen Wilkus of Alcatel-Lucent, Bo Hagerman of Ericsson and Kevin Linehan of CommScope, as well as representatives from the other member companies on 4G Americas' Board of Governors who participated in the development of this white paper.